ATMOSPHERIC WATER VAPOR TRANSPORT AND THE WATER BALANCE OF NORTH AMERICA:

PART I. CHARACTERISTICS OF THE WATER VAPOR FLUX FIELD

EUGENE M. RASMUSSON

Geophysical Fluid Dynamics Laboratory, ESSA, Washington, D.C.

ABSTRACT

The atmospheric water vapor flux over North America and the Central American Sea (Gulf of Mexico and Caribbean Sea) has been investigated for the period May 1, 1961–April 30, 1963, as part of a more general study of the water balance of these areas. Mean monthly values of the total vapor flux components are analyzed and the more important aspects of the regional vapor flux climatology are discussed and illustrated by maps and cross-sections. Additional insight into the seasonal march is obtained from the computation of the total monthly vapor flux across selected regional boundaries. Major features of the North American total vapor flux field previously described by Benton and Estoque are confirmed, but the more extensive data used in this study bring out additional significant detail, particularly over the southern United States.

Important diurnal variations are found in the flux field, particularly during the summer south of 50° N. These result primarily from diurnal variations in the average monthly wind. The characteristic features of the particularly well-organized diurnal circulation system over eastern North America and the Central American Sea are illustrated and discussed.

CONTENTS

1. INTRODUCTION

Extensive atmospheric water vapor flux data which have recently become available as part of a large-scale meteorological data-processing program are, it seems, adequate for a rather detailed study of the water vapor flux and flux divergence over North America.[1] Initial studies involving these data have pursued the following goals:

a. A detailed description of the atmospheric water vapor flux and flux divergence over the North American sector.

b. Application of these flux data, together with other hydrologic data, to regional atmospheric and terrestrial water balance studies.

c. A thorough investigation of the advantages and limitations involved in the use of water vapor flux data in large-scale water balance investigations.

This paper represents the first of a two-part summary of the more important results derived from a study of the water balance of the North American Continent and the neighboring Central American Sea (Caribbean Sea and Gulf of Mexico), covering the period May 1, 1961 through April 30, 1963 (Rasmusson [24]). The large-scale characteristics of the vapor flux field will be discussed, with emphasis on the total mean vertically integrated flux. Important diurnal variations in the flux fields have previously been noted in preliminary analyses (Rasmusson [23]), and the significant characteristics of these oscillations will be described.

The subsequent paper (Part II) will deal with the results of the flux divergence computations, and with the important topics listed under (b) and (c) above.

[1] This data-processing project was supported by the National Science Foundation under grant Nos. GP-3657 and GP-820, and directed by Prof. V. P. Starr at the Massachusetts Institute of Technology. The research described in this paper was performed while the author was on assignment at M.I.T.

A considerable number of investigations of atmospheric water vapor flux and flux divergence as they relate to the hydrologic cycle of the earth-atmosphere system, on scales ranging from less than 10^5 km.^{2} to hemispheric, have been made during the past 15 years.

Early studies by Holtzman [15] and Benton, Blackburn, and Snead [1] pointed out the importance of advected moisture in the local water balance. These were followed by a regional study over North America (Benton and Estoque [2]; Benton, Estoque, and Dominitz [3]). Many important aspects of the current study are patterned after this pioneering work.

Studies over England (Hutchings [16]), Australia (Hutchings [17]), and the Baltic Sea (Palmén [21]) have also been made, with somewhat different, but generally encouraging results. Extensive investigations of the atmospheric branch of the hydrologic cycle have been performed by members of the MIT Planetary Circulation Project, including studies by White [29], Starr and White [25], Starr and Peixoto [26], Starr, Peixoto, and Crisi [27], Peixoto and Crisi [22]. Hastenrath [11] recently investigated the water balance during 1960 over the Caribbean Sea and Gulf of Mexico.

2. DATA AND PROCEDURES

00 GMT and 12 GMT data were available for the period May 1, 1961 through April 30, 1963. 00 GMT data were also available for the period May 1958 through April 1961, but these were used only for special purposes. The basic meteorological data were obtained from the MIT General Circulation Library and consisted of mean monthly values of the following quantities

$$\bar{q}=\frac{\sum q}{N},\quad \bar{u}=\frac{\sum u}{N},\quad \bar{v}=\frac{\sum v}{N},\quad \overline{qu}=\frac{\sum qu}{N},$$

$$\overline{qv}=\frac{\sum qv}{N},\quad \overline{q'u'}=\overline{qu}-\bar{q}\bar{u},\quad \overline{q'v'}=\overline{qv}-\bar{q}\bar{v}$$

where $(\bar{\ })$ indicates a monthly mean, Σ a summation of all observations, and N the number of observations during the month at a particular Greenwich Mean Time. q is the specific humidity, u the zonal, and v the meridional wind component, and $(\ )'$ indicates a departure from the monthly mean. Throughout this paper, the term "total mean flux" will refer to $\overline{q\mathbf{V}}$, that is, the sum of the "mean flux", $\bar{q}\bar{\mathbf{V}}$ and eddy flux, $\overline{q'\mathbf{V}'}$

Data were available at the surface, 1000 mb., and at 50-mb. intervals up to 250 mb. for stations over North America and the surrounding area. Statistical estimates of q, which are available when the humidity was so low that "motorboating" occurred, were treated as actual reports.

The total water vapor content, and total horizontal mean flux of water vapor can be obtained by vertical integration, i.e.:

$$\overline{W}=\frac{1}{g}\int_{p_u}^{p_s}\bar{q}dp \tag{1}$$

$$\overline{Q_\lambda}=\frac{1}{g}\int_{p_u}^{p_s}\overline{qu}dp \tag{2}$$

$$\overline{Q_\phi}=\frac{1}{g}\int_{p_u}^{p_s}\overline{qv}dp \tag{3}$$

where $\overline{W}$ is the mean water vapor content of a column, $\overline{Q_\lambda}$ the zonal component, and $\overline{Q_\phi}$ the meridional component of the vertically integrated total mean vapor flux. No attempt was made to analyze the contribution of the eddy flux and mean flux terms separately. The column extends from the surface of the earth p_s to a pressure surface p_u above which the water vapor content is negligible. Using these integrals, we may define a 2-dimensional vector field in spherical polar coordinates

$$\overline{\mathbf{Q}}=\overline{Q_\lambda}\mathbf{i}_\lambda+\overline{Q_\phi}\mathbf{i}_\phi \tag{4}$$

where $\overline{\mathbf{Q}}$ is the vertically integrated total horizontal mean flux of water vapor above a point on the earth's surface,and $\mathbf{i}_\lambda$ and $\mathbf{i}_\phi$ are unit vectors directed positively to the east and north, respectively. $\overline{W}$, $\overline{Q_\lambda}$, and $\overline{Q_\phi}$ were computed separately for 00 GMT and 12 GMT by applying the trapezoidal rule beginning with the first even 50-mb. level above the surface and adding to this the additional contribution from the surface layer. The mean monthly surface pressure was used for p_s, the pressure at the ground. Thus it was possible to have levels with pressures higher than that of the surface in those cases where the mean monthly surface pressure was only slightly below a standard reporting level; these were excluded from consideration. Monthly means at levels having less than 10 reports were not used. Instead the data were considered missing and the value was obtained by linear interpolation between the two nearest reporting levels. Stations were considered missing if data did not extend to 700 mb. on at least 10 days of the month. Missing values at or above 500 mb. were assumed to be zero if there were no data at higher levels. The total number of reports was tabulated for each station for each month in the course of the computations. Examination of these figures indicated that missing reports below 350 mb. generally ranged between 10 and 20 percent of the total possible reports.

Separate monthly maps were plotted and hand-analyzed for $\overline{Q_\lambda}$ and $\overline{Q_\phi}$ for each of the 24 months, at both 00 GMT and 12 GMT. In addition, various auxiliary maps were plotted and analyzed in order to obtain additional information on precipitable water, diurnal flux variations, and mean seasonal patterns.

3. CHARACTERISTIC FEATURES OF THE FLUX FIELD

LARGE-SCALE FEATURES

The large-scale characteristics of the Northern Hemisphere vapor flux field during 1958 have been illustrated by Peixoto and Crisi [22]. Figures 1 and 2 are taken from their study. Their statistics show the primary source of atmospheric water vapor to be the latitude belt 15° N.–

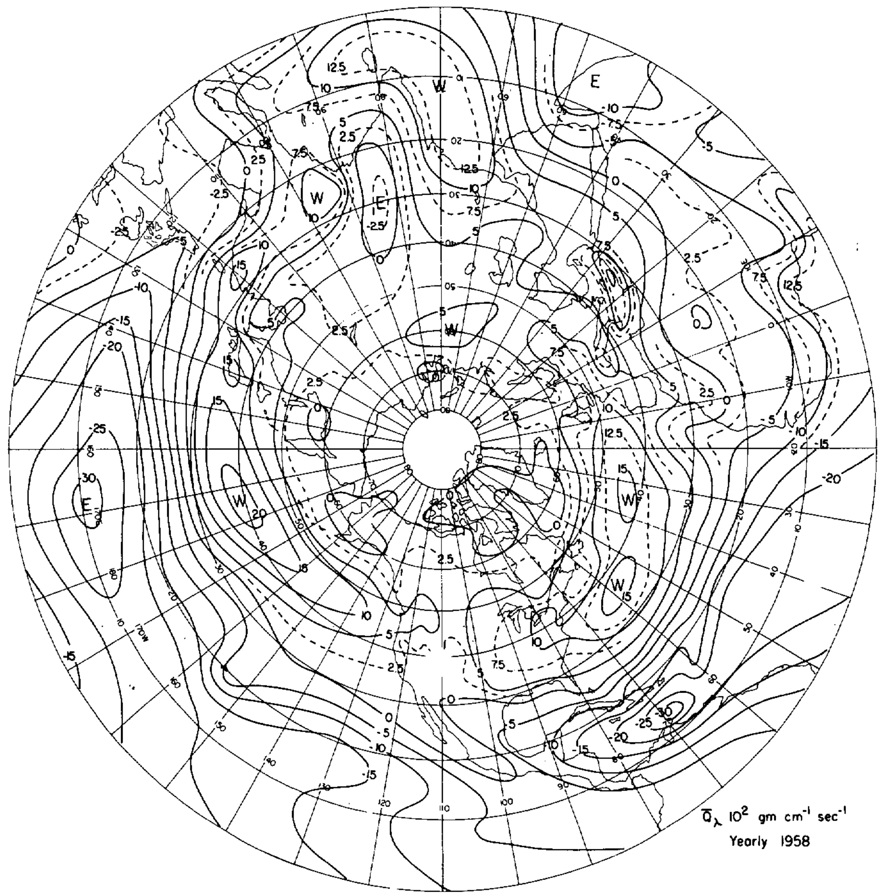

FIGURE 1.—Vertically integrated mean total zonal water vapor flux, $\overline{Q}_\lambda$, 1958. Units: 10^2 gm. (cm. sec.)$^{-1}$. (From Peixoto and Crisi [22]).

FIGURE 2.—Vertically integrated mean total meridional water vapor flux, $\overline{Q}_\phi$, 1958. (Units: 10^2 gm. (cm. sec.)$^{-1}$. (From Peixoto and Crisi [22]).

265-240 O-67—3

35° N. The mean annual southward transport from these latitudes reaches a maximum around 10° N. and the northward transport into mid-latitudes reaches a maximum around 40° N. Transient eddies transport water vapor northward at all latitudes, and are the dominant meridional transport mechanism north of 20° N. South of 20° N., the low-level mean transport dominates.

It becomes apparent, upon examination of figures 1 and 2, that significant large-scale asymmetries exist in the hemispheric pattern of the flux components; these bear an unmistakable relationship to the distribution of the continents and oceans of the hemisphere.

The most intense meridional transport occurs over the oceans. The maximum southward transport at lower latitudes is found in the vicinity of the eastern ends of the semipermanent Atlantic High and wintertime North African High, and more uniformly over the Pacific. Almost all of the mean annual northward outflow from low latitudes across 25° N. occurs in three definite areas: the southwest Pacific (south and east of Japan), the western Atlantic and Gulf of Mexico, and the Indian subcontinent and southeastern Asia. In the last area this northward outflow is associated with the Asian monsoon and is primarily a summertime phenomenon. The regions of northward flux in the western Pacific and western Atlantic-Gulf of Mexico mark the southwestern extremities of the major oceanic cyclone belts. Since the mean annual northward transport associated with the Asian monsoon becomes insignificant north of 35° N., it follows that the primary moisture transport to latitudes above 35° N. is accomplished in the oceanic cyclone belts of the Atlantic and Pacific. These are found at progressively higher latitudes as one moves eastward across the oceans.

The major features of the flux fields over North America during the period of our investigation are illustrated in figures 3 through 8. Two main currents are observed to enter the continent. One is associated with the northeastern extremity of the Pacific cyclone belt, and crosses the Pacific Coast, generally between 40° and 55° N. It then weakens rapidly and finally merges with the second, more intense, current east of the Continental Divide. The second major inflow area, associated with the southwestern extremity of the Atlantic cyclone belt, crosses the Gulf Coast, and is particularly intense during the summer months. This is essentially the pattern found in 1950 by Benton and Estoque [2].

MEAN MONTHLY FLUX—CENTRAL AMERICAN SEA

Seasonal variations in the vapor flux will now be considered in greater detail. For this purpose, it is convenient to consider separately the larger regions which were designed for later use in conjunction with flux divergence computations. These regions, shown in figure 9, are (a) the Caribbean Sea, (b) the Gulf of Mexico, (c) the two areas comprising the United States and southern Canada, and (d) northern North America. The boundary of each of these areas is broken into sections, whose end points are denoted by circles. The annual flux across each section of boundary, and the annual flux divergence from each area are shown in figure 9.

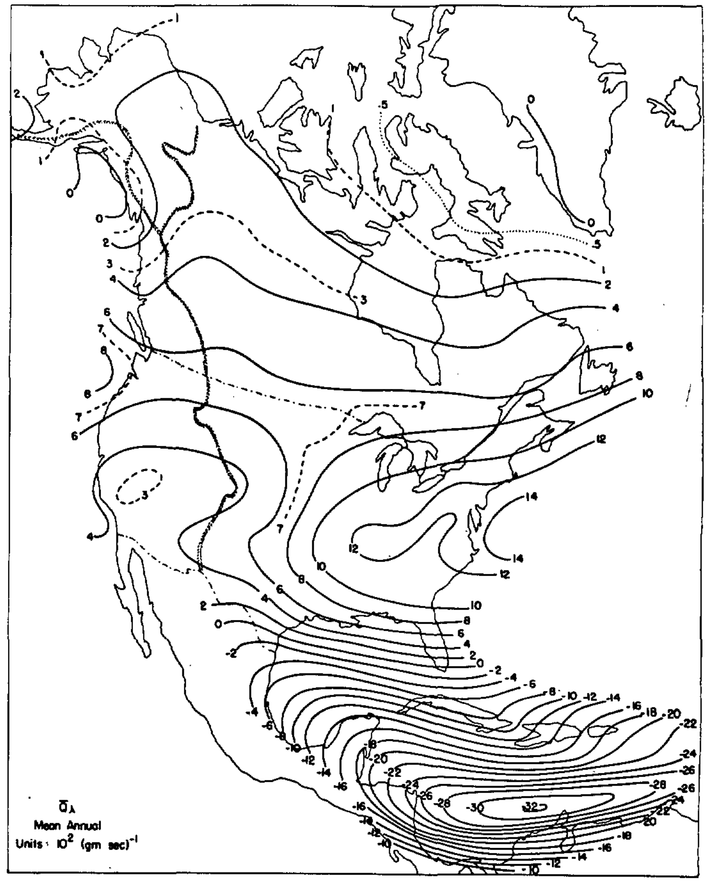

FIGURE 3.—Mean annual vertically integrated total zonal water vapor flux. May 1961–April 1963. Units: 10^2 gm. (cm. sec.)$^{-1}$.

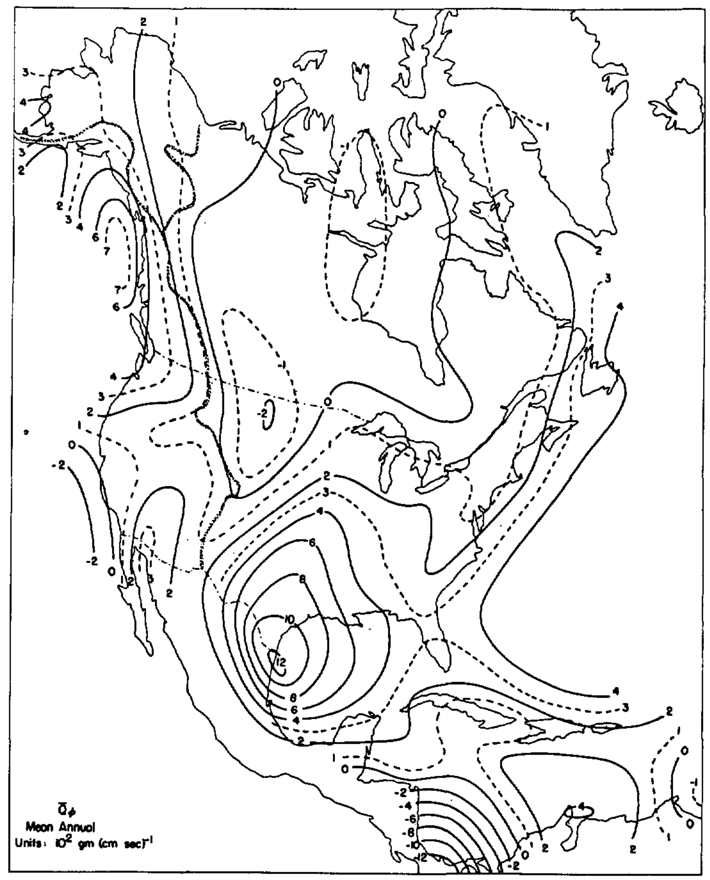

FIGURE 4.—Mean annual total meridional water vapor flux, May 1961–April 1963.

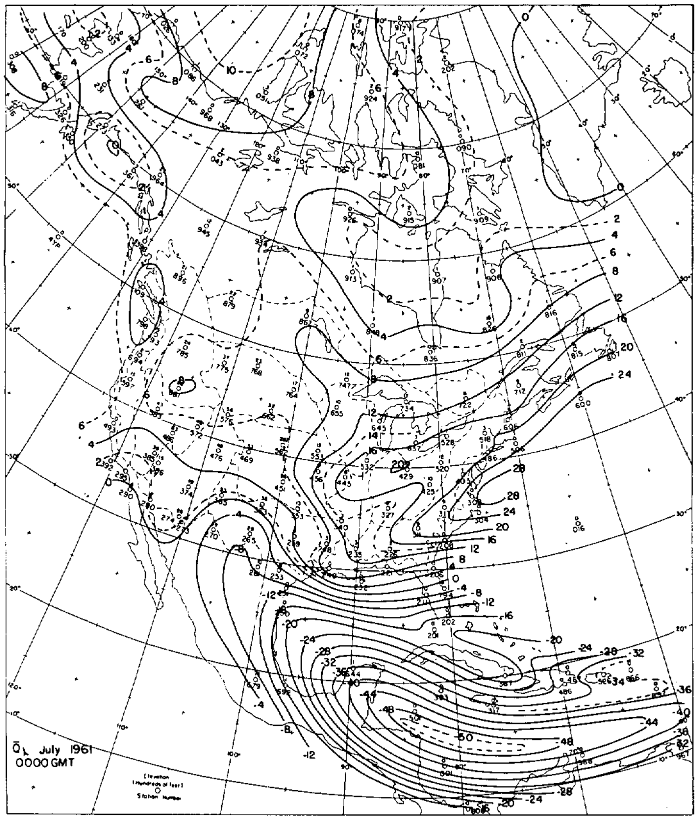

FIGURE 5.—Mean monthly vertically integrated total zonal water vapor flux, July 1962. Units: 10^2 gm. (cm. sec.)$^{-1}$.

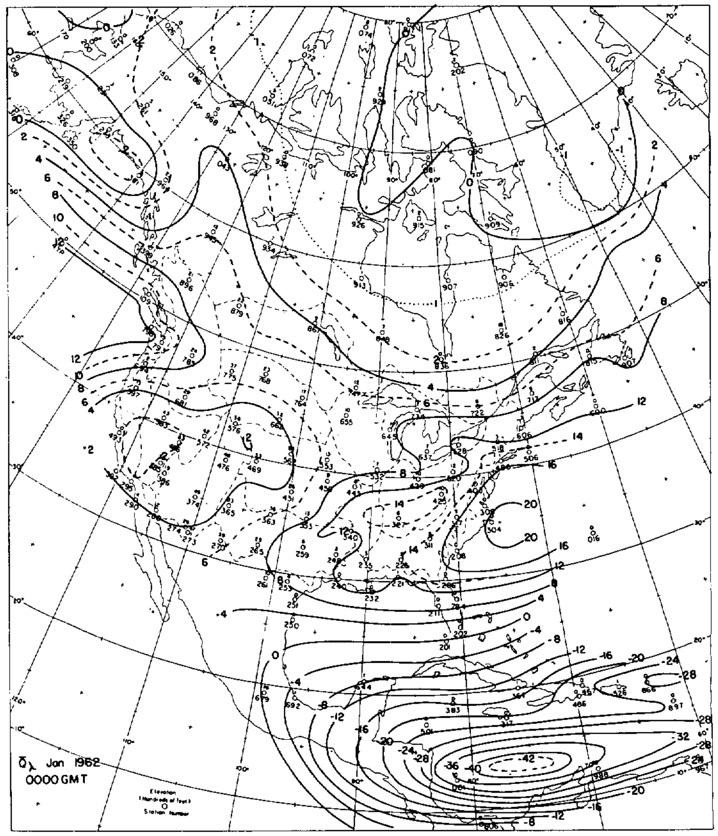

FIGURE 7.—Mean monthly vertically integrated total zonal water vapor flux, January 1962. Units: 10^2 gm. (cm. sec.)$^{-1}$.

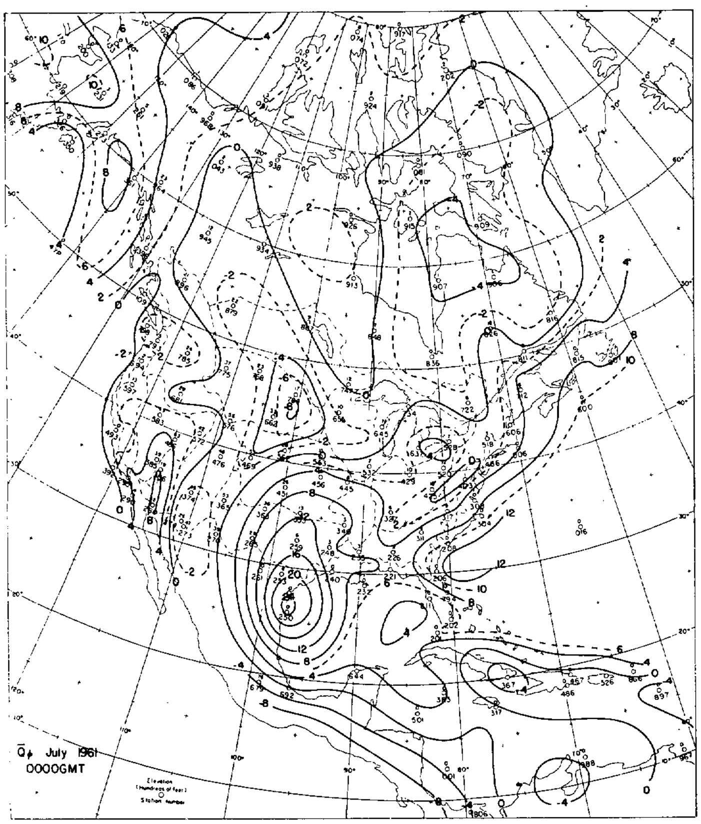

FIGURE 6.—Mean monthly vertically integrated total meridional water vapor flux, July 1962.

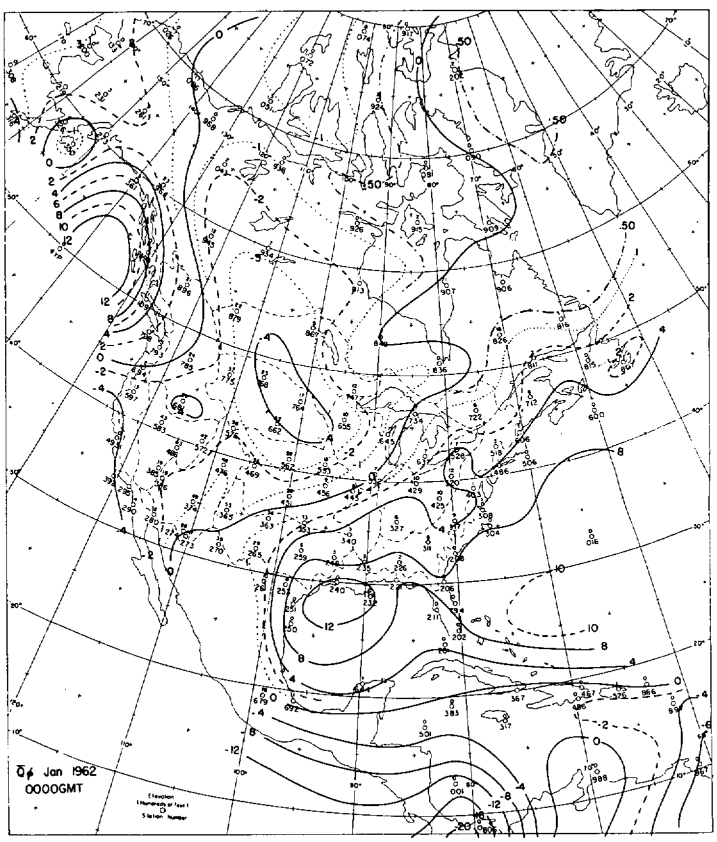

FIGURE 8.—Mean monthly vertically integrated total meridional water vapor flux, January 1962.

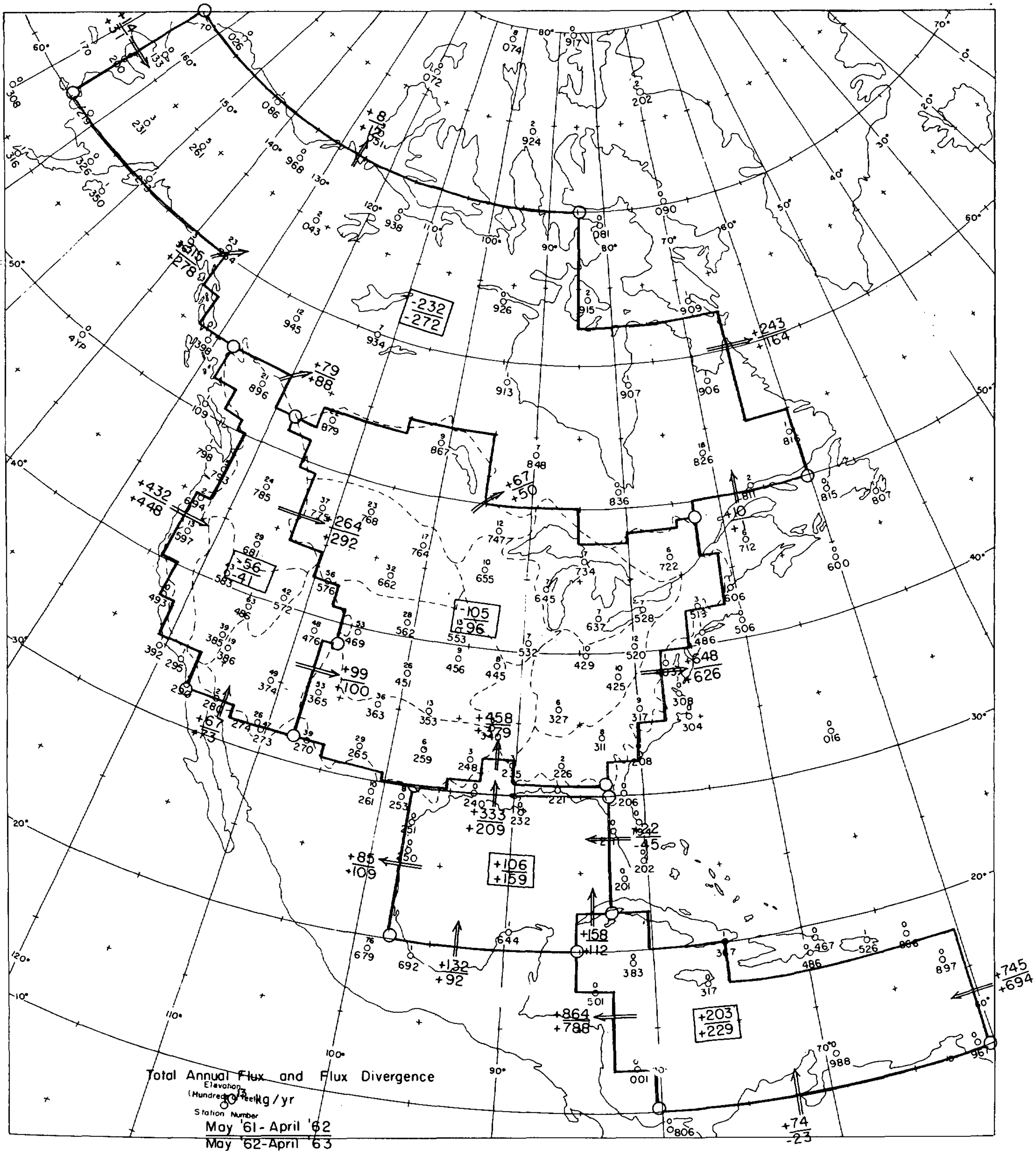

FIGURE 9.—Total net annual flux across selected boundaries. Upper number is total for May 1961–April 1962; lower number for May 1962–April 1963. Flux is positive in the direction of the arrow. Total annual flux divergence is shown for each enclosed area. Units: 10^{13} kg. yr.$^{-1}$

The ocean areas comprising the Gulf of Mexico and Caribbean Sea, referred to by Wüst [30] as the Central American Sea, play a key role in the water balance and overall climate of much of southern and eastern North America. This region together with the western Atlantic comprises one of the three Northern Hemisphere regions of major northward moisture flux across 20° N. and 30° N. The entire area lies between 10° N. and 30° N. and thus straddles the latitudes from which huge amounts of latent heat energy are exported. The western portions of the Central American Sea act as a distribution zone for the moisture entering from the Atlantic and added by excess evaporation within the region. Part of this moisture flows northward into eastern North America, but the flux analyses, which are based on the stations shown in figure 9, indicate that most of the outflow takes place in a westerly to southwesterly direction across the western boundary of the Caribbean (See figs. 4, 6, 8, and 9). Lesser amounts of moisture cross the mountains of Mexico and the South American coasts in a direction which varies with the season (see figs. 10 and 11). Certain features of the flux within this region have previously been discussed by Hastenrath [11] and Rasmusson [24].

The mean monthly moisture flux across the lines defining the eastern and western boundaries of the Central American Sea is shown in figure 10, and the flux across the northern and southern boundaries is shown in figure 11. As noted in figure 9, the eastern boundary is considered to extend from near Trinidad to western Cuba. The general characteristics of the vertical distribution of the influx from the Atlantic can be obtained from the cross sections along 80° W. (figs. 12 and 13). As pointed out by Hastenrath [11], the bulk of the transport into the Caribbean Sea takes place below 800 mb. with a maximum around 950 mb. during both summer and winter. At 80° W., the boundary between easterly and westerly flow at the surface is found just south of 30° N. in both January and July. However, this boundary shifts southward during the winter in the Gulf of Mexico, with the displacement increasing as one progresses westward. This accounts for the seasonal change in sign of the average flux across the meridional boundaries of the Gulf of Mexico. Even in winter, however, the vertically integrated flux in the southern portion of the basin is directed westward.

The strong inflow through the eastern Caribbean boundary, observed during every month, exhibits a double maximum, the more intense one occurring in July and a much weaker maximum occurring in December or January. The July maximum coincides with the occurrence of high values of $\overline{q}$ and a northward flux component. The winter maximum coincides with near minimum values of $\overline{q}$ and a southward flux component. Figures 12 and 13 indicate no essential difference in the vertical flux distribution at the time of the two maxima; thus the winter maximum is primarily the result of an increase in the mean winds. The outflow across the western boundary shows essentially the same pattern and magnitude as the eastern inflow.

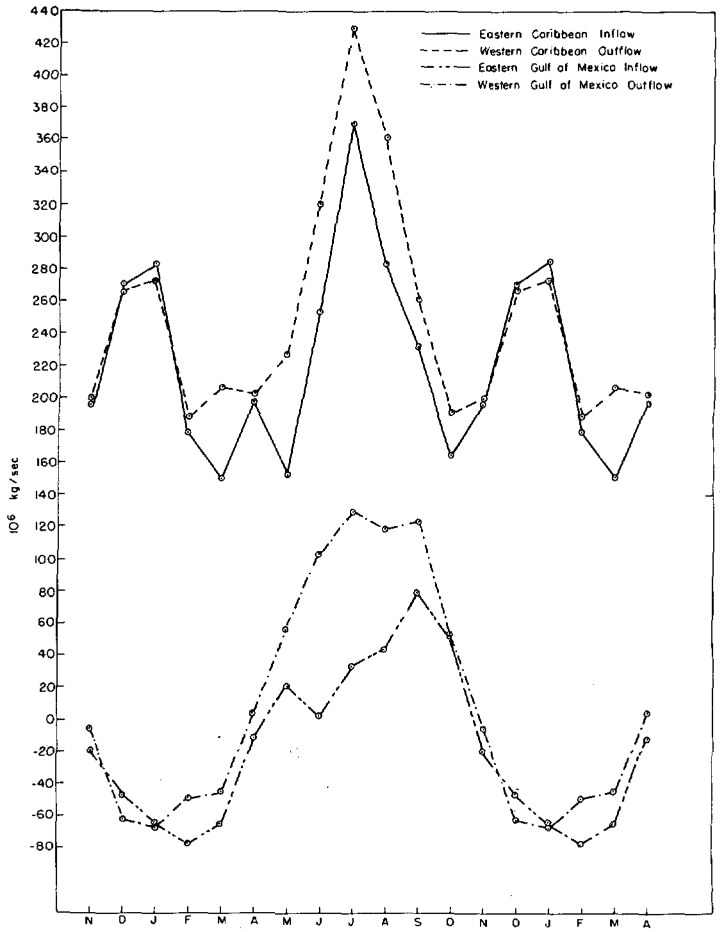

FIGURE 10.—Mean monthly vertically integrated total water vapor flux across various eastern and western sections of the boundary around the Gulf of Mexico and Caribbean Sea, May 1961–April 1963. Units: 10^6 kg. sec.$^{-1}$

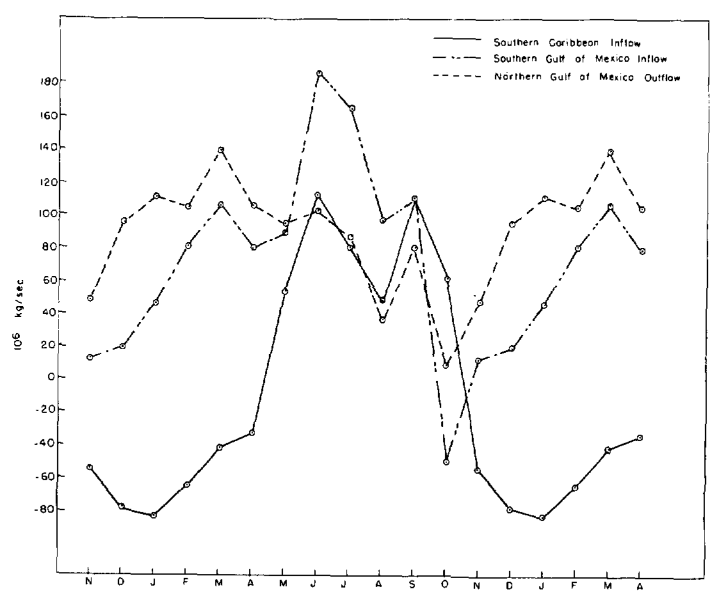

FIGURE 11.—Same as figure 10 for various southern and northern sections of the boundary.

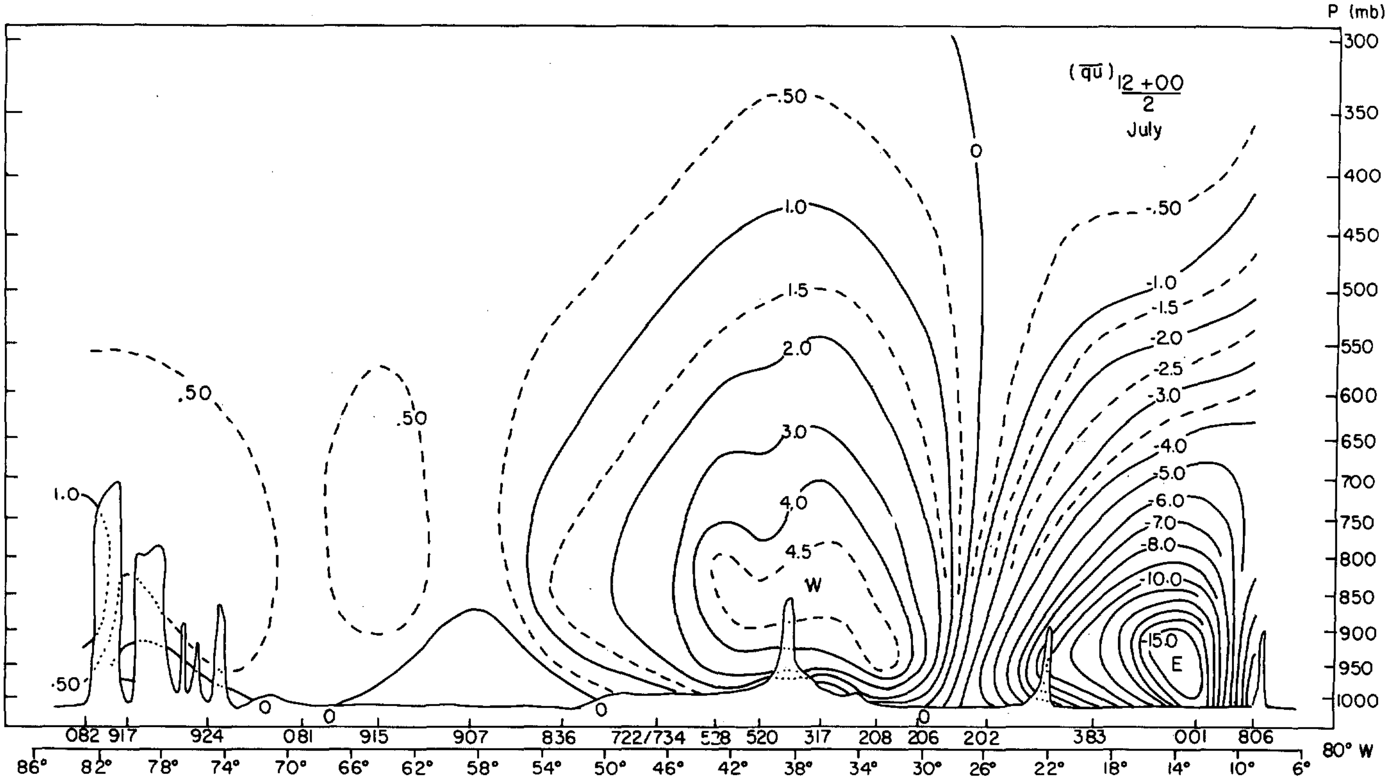

FIGURE 12.—Mean total zonal water vapor flux, 10° N.–83° N. at 80° W., July 1961–62. Units: gm. (cm. mb. sec.)$^{-1}$.

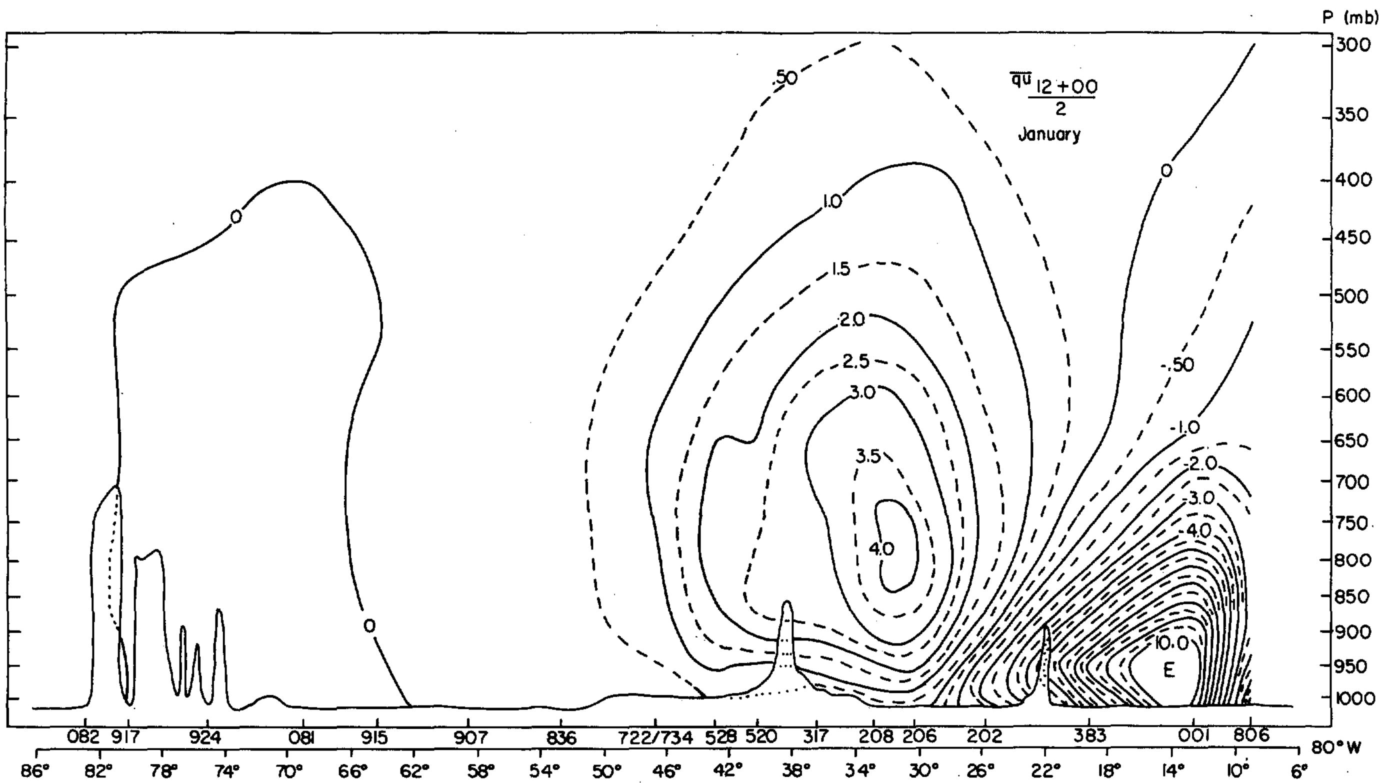

FIGURE 13.—Same as figure 12, but for January 1962–63.

The flux across the southern boundary of the Caribbean exhibits a seasonal shift in direction, northward from May through October, and southward during the remainder of the year. The peak northward flux, which closely coincides with the two computed Caribbean precipitation maxima (to be discussed in Part II), occurs in June and September.

A strong seasonal change is also noted in the magnitude of the northward flux across the southern boundary of the Gulf of Mexico. There is some indication of the twin maxima found on the South American coast, although the June maximum is dominant. Two years of data are probably not sufficient to establish the reality of the weaker maximum. Similarly, preliminary examination of data for October 1958, 1959, and 1960 does not substantiate the sharp minimum observed in October 1961 and 1962.

The transport across the northern boundary of the Gulf of Mexico shows the least seasonal variation, although a maximum northward flux appears in spring, and a minimum in late summer or fall. The values for September may be affected by the occurrence of hurricane Carla, which struck the Texas coast in September 1961. A sharp and possibly anomalous minimum of northward flux is again observed in October. One should not equate the flux across this boundary, which extends only to 97.5° W., with the flux from the Gulf of Mexico into the United States, as during summer a large part of the moisture crossing the western boundary of the Gulf of Mexico ultimately enters the United States between 97.5° W. and the Rocky Mountains. This is quite apparent from figure 14.

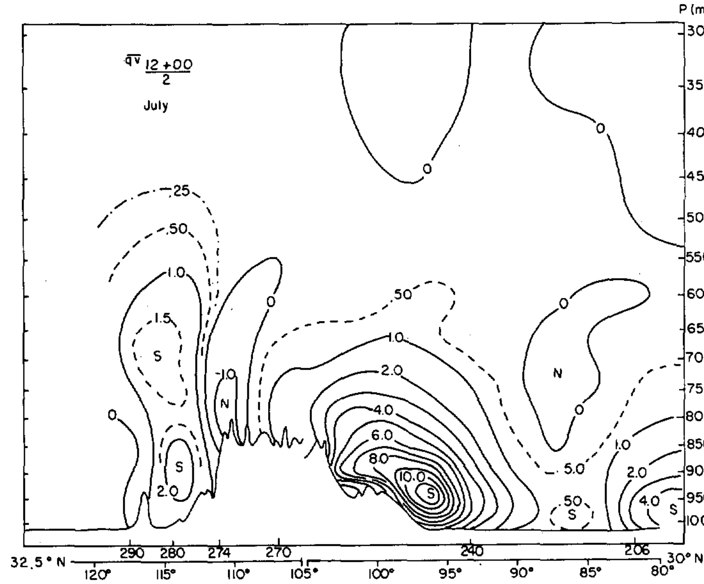

FIGURE 14.—Mean total meridional water vapor flux: 30° N.; 80° W.–105° W. and 32.5° N.; 105° W.–117.5° W. July 1961–62. Units: gm. (cm. mb. sec.)$^{-1}$.

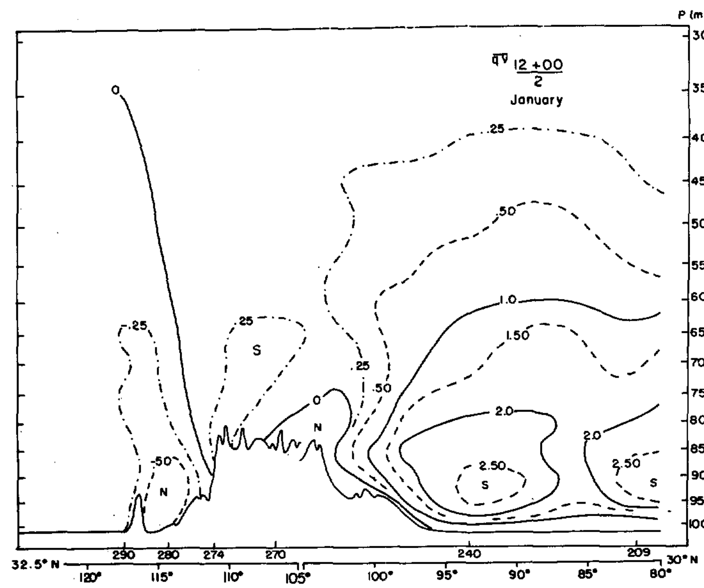

FIGURE 15.—Same as figure 14, but for January 1962–63.

MEAN MONTHLY FLUX—NORTH AMERICA

Northern North America.—The mean monthly moisture flux across the boundaries of this region is illustrated in figure 16; mean annual values are shown in figure 9. The southern inflow consists of the inflow through the three continental sections of the southern boundary.

Also shown in figure 16 is the computed value of $\overline{P-E}$ (the difference between total precipitation and total evapotranspiration over the area) which is obtained from a computation of the vapor flux divergence. The reliability of such estimates will be discussed in detail in Part II of this summary. This will include comparisons of values obtained from the water balance equation with estimates, such as those of Budyko [6], which are based primarily on heat budget considerations. $\overline{P-E}$ is included on the figure in order to facilitate the discussion of the relative importance of the various boundary fluxes to the average water balance of the total area, and is believed to be quite adequate for this purpose.

The mean annual flux across the northern boundary was directed into the Arctic Ocean, and was quite small. It is, of course, of local importance, but was of significance to the mean water balance of the total area only during July and possibly in August. The mean flux across the west coast of Alaska was also of minor importance to the annual mean water balance of the total area, amounting to only 10 percent of $\overline{P-E}$. However, it was of some importance on a mean monthly basis during the summer months. The sum of the inflow through these two boundaries was of even less importance to the water balance of the total area. Thus, the mean water balance for northern North America is essentially determined by the flux across the Pacific, southern, and Atlantic boundaries.

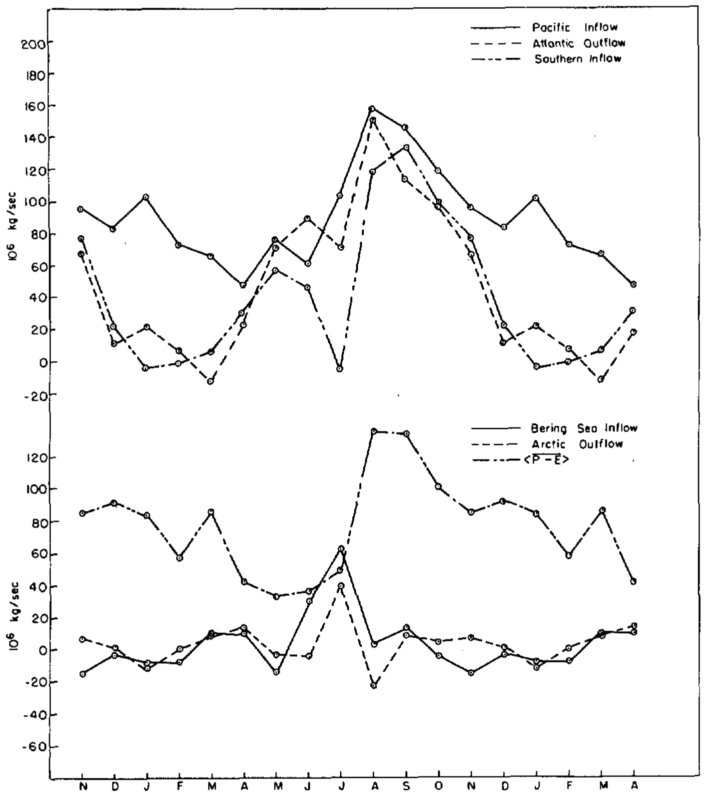

FIGURE 16.—Mean monthly vertically integrated water vapor flux across various sections of the boundary of northern North America, May 1961–April 1963. Units: 10^6 kg. sec.$^{-1}$

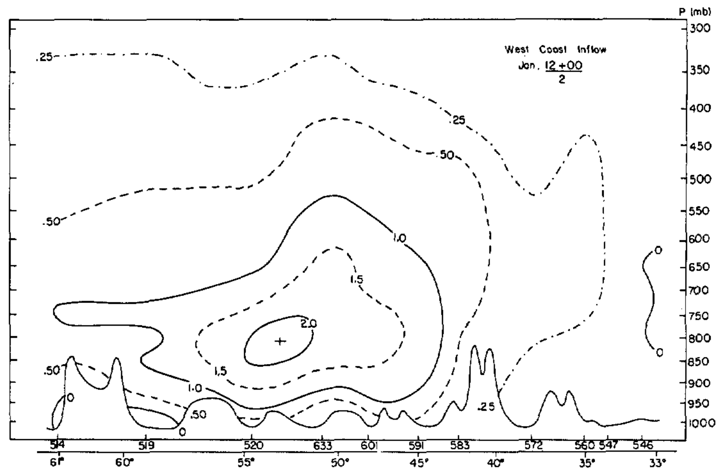

FIGURE 18.—Same as figure 17, but for January 1962–63.

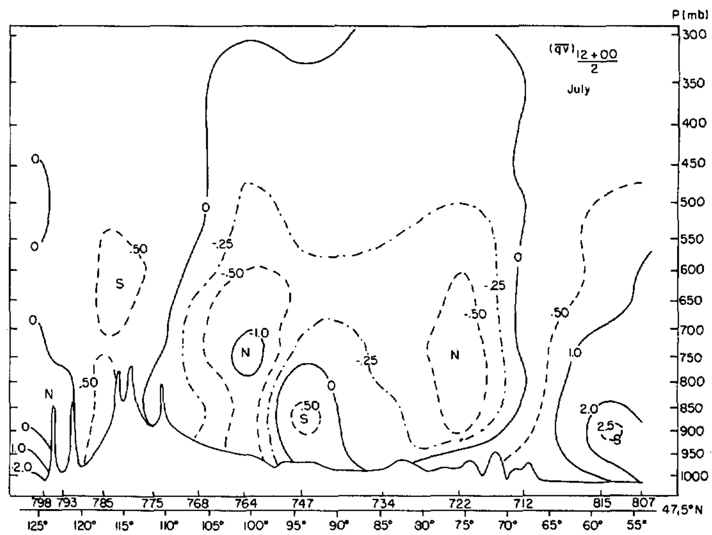

FIGURE 19.—Mean total meridional water vapor flux across 47.5° N.; 55° W.–125° W., July 1961–62. Units: gm. (cm. mb. sec.)$^{-1}$.

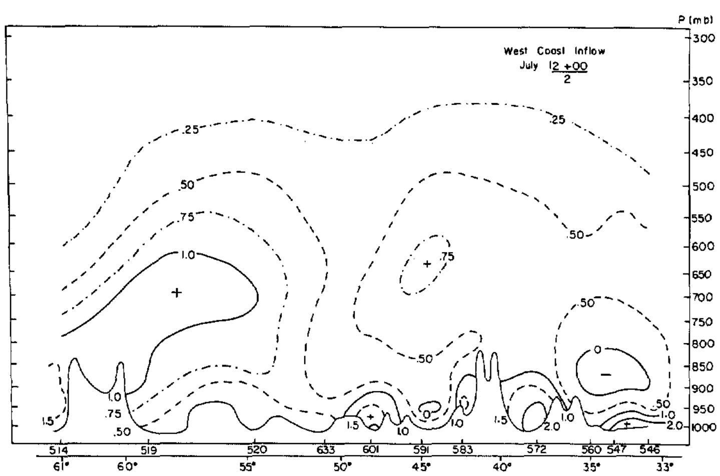

FIGURE 17.—Mean total water vapor influx—west coast of North America. 32.5° N.–61° N., July 1961–62. Units: gm. (cm. mb. sec.)$^{-1}$.

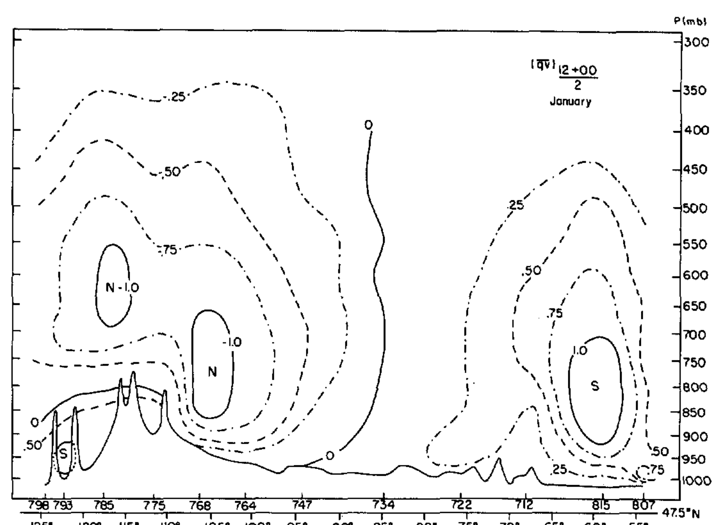

FIGURE 20.—Same as figure 19, but for January 1962–63.

Some idea of the vertical distribution of the Pacific inflow can be obtained from figures 17 and 18. The pattern is rather flat in both winter and summer, usually with a diffuse maximum between 700 and 850 mb. The relation of this maximum to the Pacific cyclone belt has been discussed previously.

The mean monthly Pacific inflow reaches a maximum in August, one month after the local maximum on the western Alaskan coast. The local flux maximum apparently continued to migrate southward during the winter, reaching the California coast in February 1962 and April 1963, the two months of heaviest precipitation in that area. Thus the movement of the local flux maximum appears to coincide with the seasonal southward shift of the local precipitation maximum, and, like the local precipitation maximum, does not appear to return northward in spring.

The vertical structure of the Atlantic outflow can be implied from figures 12 and 13. This region lies north of the main belt of eastward transport during the entire year. A westward transport into the continent is found north of 60° N. during the winter, possibly the result of westward flow on the northern side of the intense oceanic low pressure areas. The maximum eastward flux is again found in August.

The inflow across the southern boundary (figs. 19 and 20) follows a seasonal pattern similar to that of the Atlantic outflow. A northward low-level eddy flux, which is strongest during summer, accounts for a significant portion of the mean annual inflow through this boundary (Peixoto and Crisi [22]).

United States-Southern Canada.—The characteristics of the flux over this area, and across its boundaries, are illustrated in figures 21 and 22 and on the various cross sections. The more important features of the flux field will be briefly noted.

Most of the inflow from the Pacific Ocean crosses the west coast north of 40° N. in winter and 50° N. in summer, and enters the area from the west and northwest. As first noted by Benton and Estoque [2], this appears as a diffuse high-level inflow on mean monthly charts, particularly in the region east of the Continental Divide. The tendency for a relatively large part of the inflow to take place above 850 mb. is apparently the result of the high terrain of the Pacific coastal regions, since the eastern Atlantic counterpart of this current shows a strong low-level influx well into central Europe (Peixoto and Crisi [22]).

Charts from Peixoto and Crisi [22], and additional cross sections (not shown here), show that the mean total flux through the northern boundary, between the Appalachian and Rocky Mountains, is usually the difference between a southward mean flux and a northward eddy flux.

The inflow through the southern boundary is illustrated in figures 14 and 15. The differences between the January and July inflow, as well as the summertime diurnal variations (fig. 32), are quite pronounced. Additional cross sections (not shown here) and previous studies have established that the January inflow is primarily an eddy transport, while the July inflow is due primarily to transport by the mean monthly wind. The strong and persistent northward flux in summer around the western end of the subtropical High results in a concentrated region of intense inflow over Texas.

Rather interesting secondary maxima are found at the northern end of the Gulf of California. The July northward flux maximum, which extends to relatively high levels, is stronger above 700 mb. than the inflow east of the Rockies. Mean monthly data from Yuma showed the inflow to be from the southwest below 800 mb. However, in the region from 750 to 500 mb. the flow was from the south to south-southeast. The flux vector at these levels showed a shift from the southwest and a sharp increase in magnitude between June and July. A somewhat smaller decrease in magnitude and a shift back to a southwesterly direction was observed between August and September. The wintertime southward component developed first in the low levels in October, and was established at all levels by November. The northward component was reestablished at the higher levels in February, and worked its way to the surface by May.

The total vertically integrated mean monthly flux across various portions of the boundary, and across the Continental Divide, is illustrated in figures 21 and 22. Separate values for 00 GMT and 12 GMT have been shown in order to illustrate the effects of the diurnal flux variation, which are discussed in detail in section 4.

The most pronounced flux differences between 00 GMT and 12 GMT are found in summer along the eastern, western, and Gulf Coast boundaries. No significant systematic differences are apparent in the average for the northern boundary. Estimates of the flow across the Continental Divide indicate the eastward flux may be slightly stronger at 00 GMT.

The mean flux divergence over the area (fig. 22, upper) also shows a marked diurnal variation, produced primarily by a lack of balance between increased 12 GMT Gulf Coast inflow (fig. 22, lower left), increased 12 GMT east coast outflow (fig. 22, lower right), and decreased 12 GMT west coast inflow (fig. 21, lower left). The magnitude and the sign of this imbalance changed throughout the year, resulting in lower values of divergence at 12 GMT from January through June, much higher values from June through September, with little difference from October through December. However, variations during comparable months of the 2-yr. period differed considerably, sometimes even in sign; thus analysis of a longer period is required in order to establish a stable pattern.

The total annual flux across the boundaries is summarized in table 1. Also given for comparison is the resulting computed flux divergence.

Note that year-to-year variations in the predominantly zonal inflow and outflow were small during this 2-yr. period, but changes in the flux divergence, and in the meridional flux from the Gulf of Mexico, were significant.

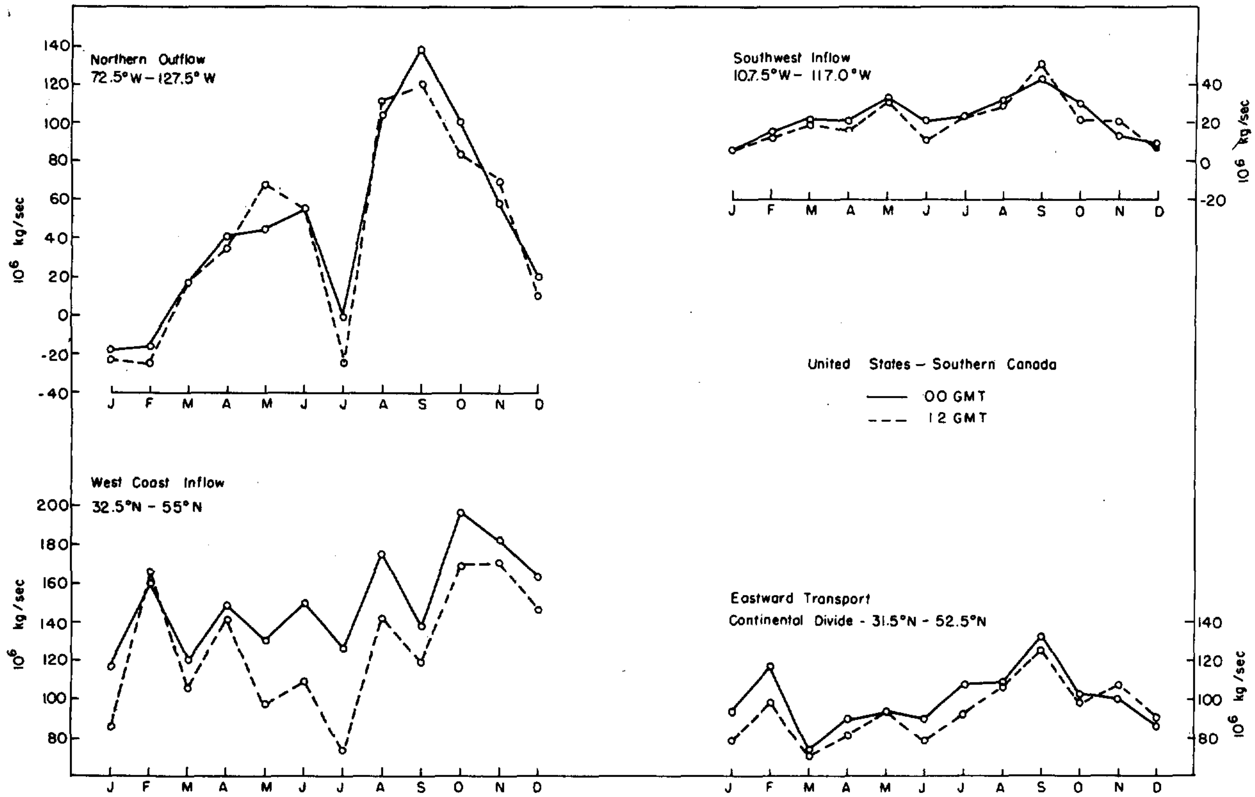

FIGURE 21.—Mean monthly vertically integrated water vapor flux across various sections of the boundary of the United States and southern Canada, May 1961–April 1963.

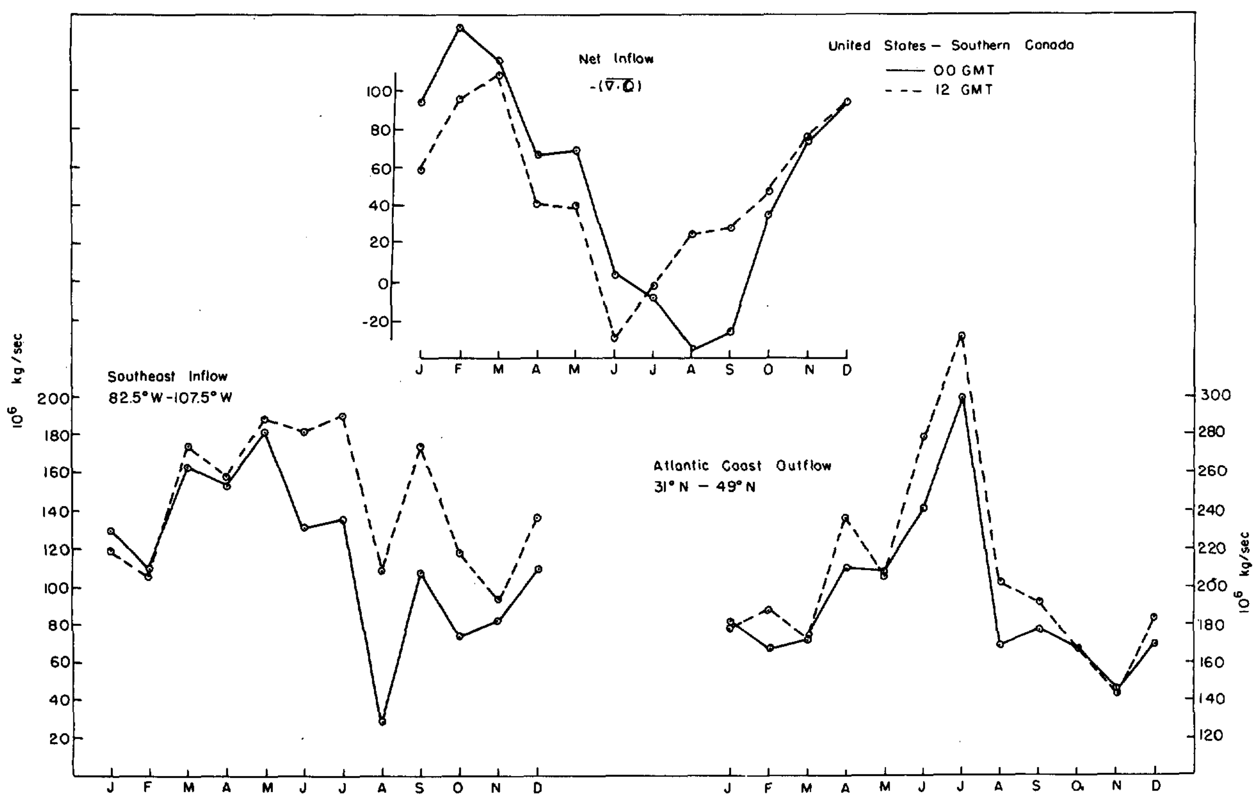

FIGURE 22.—Same as figure 21 for additional sections of the boundary of the United States and southern Canada. Also shown is the net mean monthly inflow into the area.

TABLE 1.—*Total annual mean flux and flux divergence for the United States and southern Canada. Units: 10^{13} kg./yr.*

	Time (GMT)	1961–62	Mean	1962–63	Mean
West Coast inflow	00	471	432	482	448
	12	392		415	
Southwest inflow	00	70	67	74	73
	12	64		72	
Gulf of Mexico inflow	00	418	458	329	379
	12	498		429	
Atlantic outflow	00	604	648	616	626
	12	692		636	
Northern outflow	00	140	146	149	138
	12	151		128	
$\nabla \cdot \overline{\mathbf{Q}}$	00	215	163	120	136
	12	111		152	

4. DIURNAL VARIATIONS IN THE FLUX FIELD

PREVIOUS STUDIES

Relatively little information is available on the mean monthly diurnal variations of wind and humidity in the troposphere, as most previous studies have been limited to individual stations or to scattered data from rather restricted areas. However, the existence of significant diurnal wind variations, under certain conditions and over certain regions, is well known. The complex local land-sea breeze systems have been widely studied. The existence of mountain-valley wind systems (Defant [8]) may have pronounced effects at some stations in the mountainous regions of North America. Low-level nocturnal wind maxima have been investigated by Gerhardt [9], Hoecker [13, 14], Izumi and Barad [18], Izumi [19], Kaimal and Izumi [20], and others, and theories on their existence and behavior have been proposed by Blackadar [4] and Wexler [28]. Curtis and Panofsky [7] found important diurnal variations in the mean large-scale vertical motion field over the midwestern United States during a 10-day period in July. These appeared to be related to the nocturnal thunderstorm maximum of the Great Plains. Bleeker and Andre [5] found significant diurnal changes in the mean divergence field in the same general area during August. These two investigations suggest the possibility of significant diurnal variations in the vapor flux divergence as well as in the vapor flux itself. Harris [10] evaluated the first two harmonics of the tropospheric diurnal wind variations during three summer months at Washington, D.C., and found first harmonic components which exceeded 1 m. sec.$^{-1}$, and second harmonic components which exceeded 0.4 m. sec.$^{-1}$ Hering and Borden [12], in an investigation which clearly indicates the necessity for dealing with this problem, found prominent diurnal variations in the mean monthly summer wind field over the central United States.

Early confirmation of the existence of significant differences between the mean 00 GMT and 12 GMT flux during the summer (Rasmusson [23]) lead to a more detailed investigation of this phenomenon. The summer months, when the oscillations reach their maximum, and particularly the month of July, were chosen for the most detailed study. Data consisted of regular 00 GMT and 12 GMT observations and a limited number of 06 GMT and 18 GMT observations from Tinker Air Force Base and Fort Worth.

Only small diurnal variations of $\overline{q}$ were found during July, while large diurnal variations were found in the mean monthly wind vector. Furthermore, where diurnal variations were important, the diurnal variation in $\overline{q'\mathbf{V}'}$ was found to be small compared with the total mean flux variation. Consequently, the most prominent diurnal variations are in general due to diurnal variations in the monthly averaged wind, rather than in the specific humidity.

DIURNAL CIRCULATION SYSTEM OF NORTH AMERICA AND THE CENTRAL AMERICAN SEA

The characteristics of the diurnal variations of $\overline{q\mathbf{V}}$ and $\overline{\mathbf{V}}$ at various heights were investigated. Hodographs were plotted for July 1961 and 1962, for 77 stations located in southern Canada, the United States, and in the Gulf of Mexico-Caribbean Sea region.

The important characteristics of the July oscillations can be described by dividing the area into several regions, in each of which the hodographs exhibit broadly similar characteristics. These regions are illustrated on figure 31.

Typical hodographs from Region A are shown in figure 23. A comparison of the $\overline{q\mathbf{V}}$ and $\overline{\mathbf{V}}$ hodographs for Guadeloupe and St. Maarten clearly show the dominant effect of the wind in producing the diurnal flux variations. Furthermore, these variations in the wind are by no means small when compared with mean monthly values, nor are they limited to the lower levels, but often extend at least into the upper troposphere. On the other hand, the $\overline{q\mathbf{V}}$ oscillation decreases with height in response to the decrease in $\overline{q}$. Thus the vapor flux oscillations above 850 mb. are less important than those in the lower layers, but are by no means negligible. The veering of $\overline{q\mathbf{V}}$ between 00 and 12 GMT, and the accompanying increase in southerly flow, are the typical features of this region.

Region B consists of the area of northeasterly surface flow in the western Caribbean, which is illustrated by the San Andres hodographs (fig. 24). The backing of the flux vector from 00 GMT to 12 GMT at levels below 700 mb. constitutes the main difference between this hodograph and the hodographs of region A. Comparison of the $\overline{q\mathbf{V}}$ and $\overline{\mathbf{V}}$ hodographs again verifies the importance of the wind variation in producing the vapor flux oscillation. Note the shift from a backing to a veering wind change

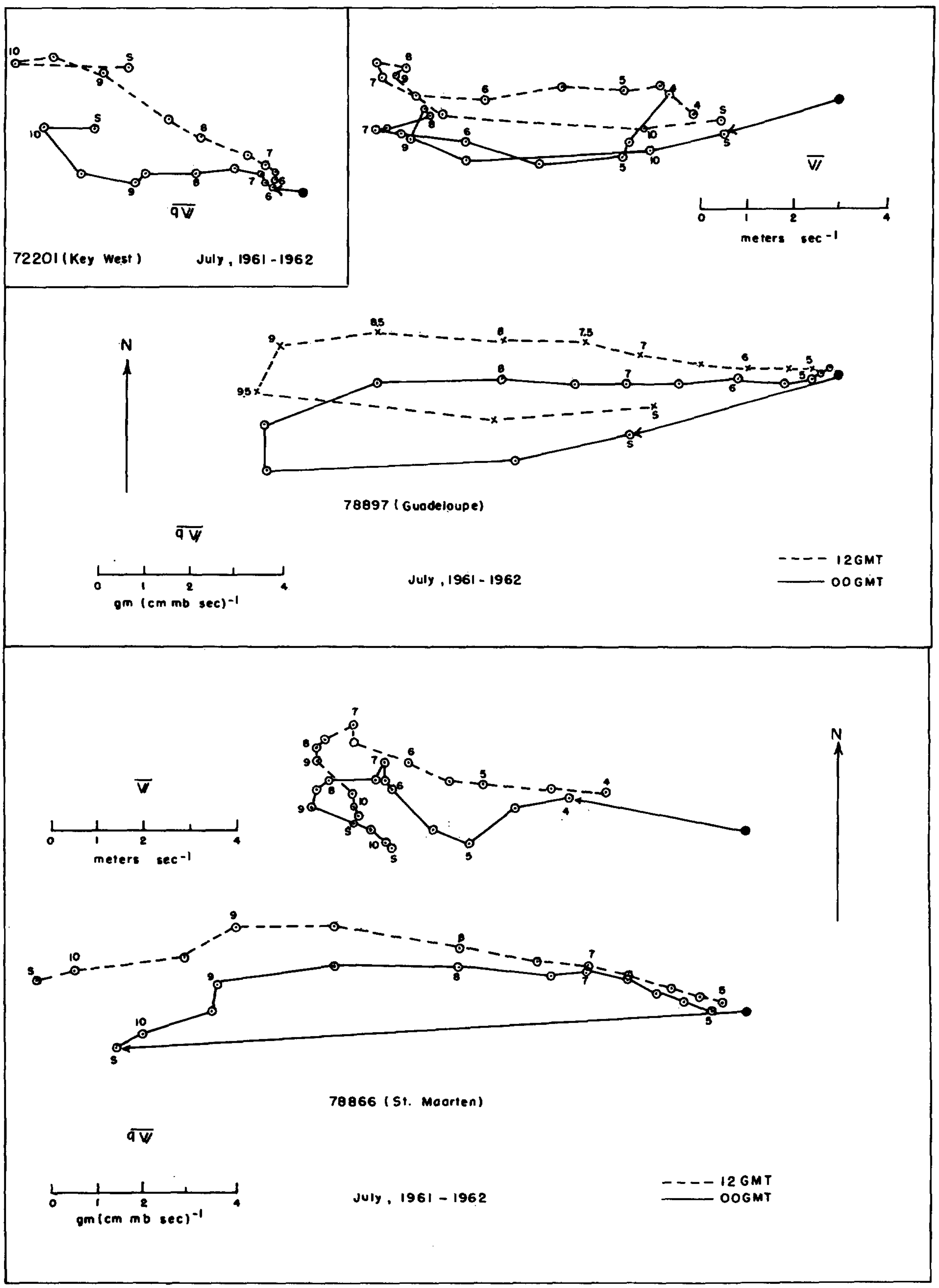

FIGURE 23.—Hodographs $\overline{qV}$ and $\overline{V}$ for Key West, Guadeloupe, and St. Maarten, July 1961–62. Origin denoted by solid circle. Pressure given in hundreds of millibars. "S" denotes surface value.

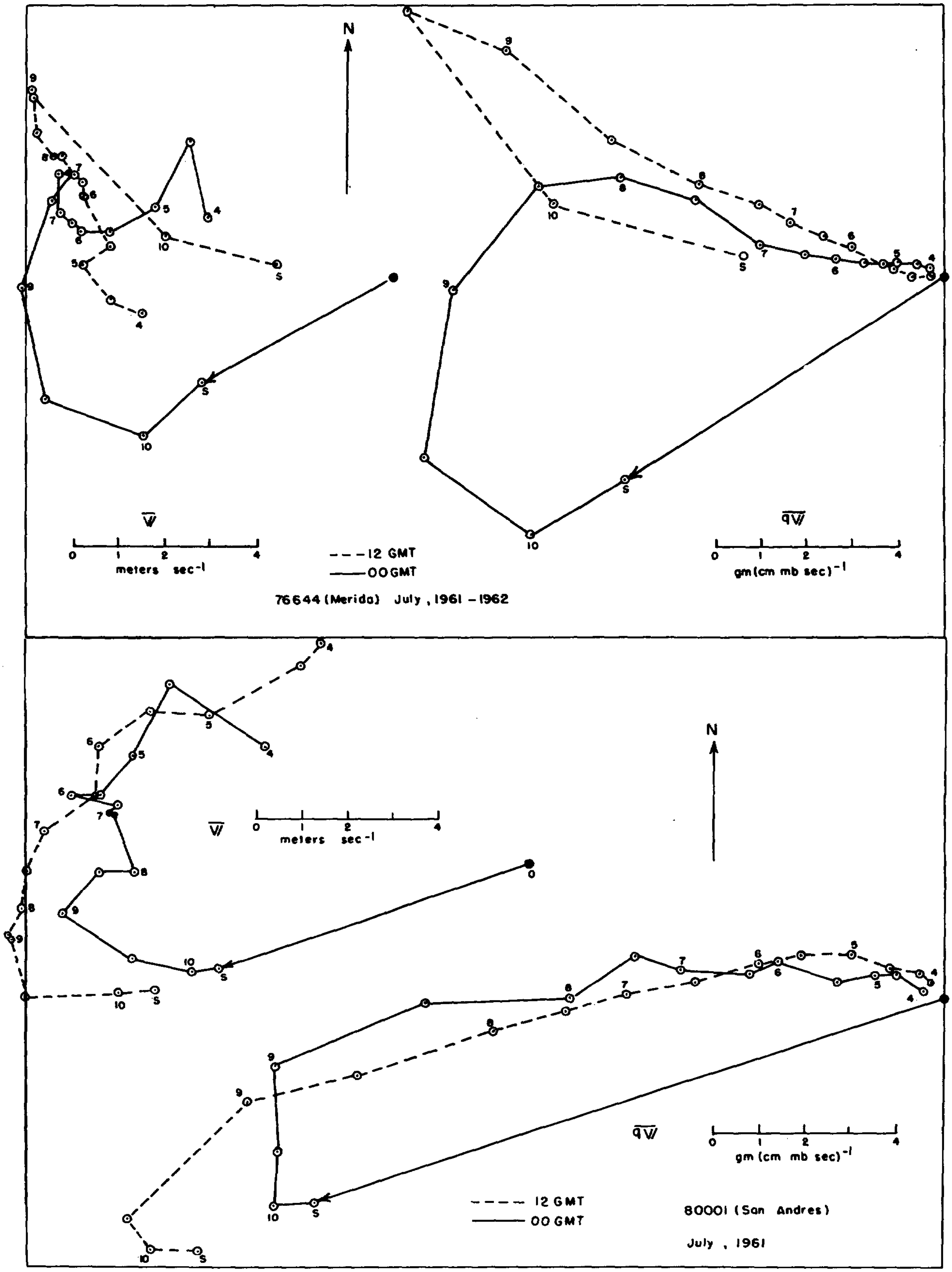

FIGURE 24.—Hodographs: $\overline{q\mathbf{V}}$ and $\overline{\mathbf{V}}$ for Merida, July 1961–62, and San Andres, July 1961. Origin denoted by solid circle. Pressure given in hundreds of millibars. "S" denotes surface value.

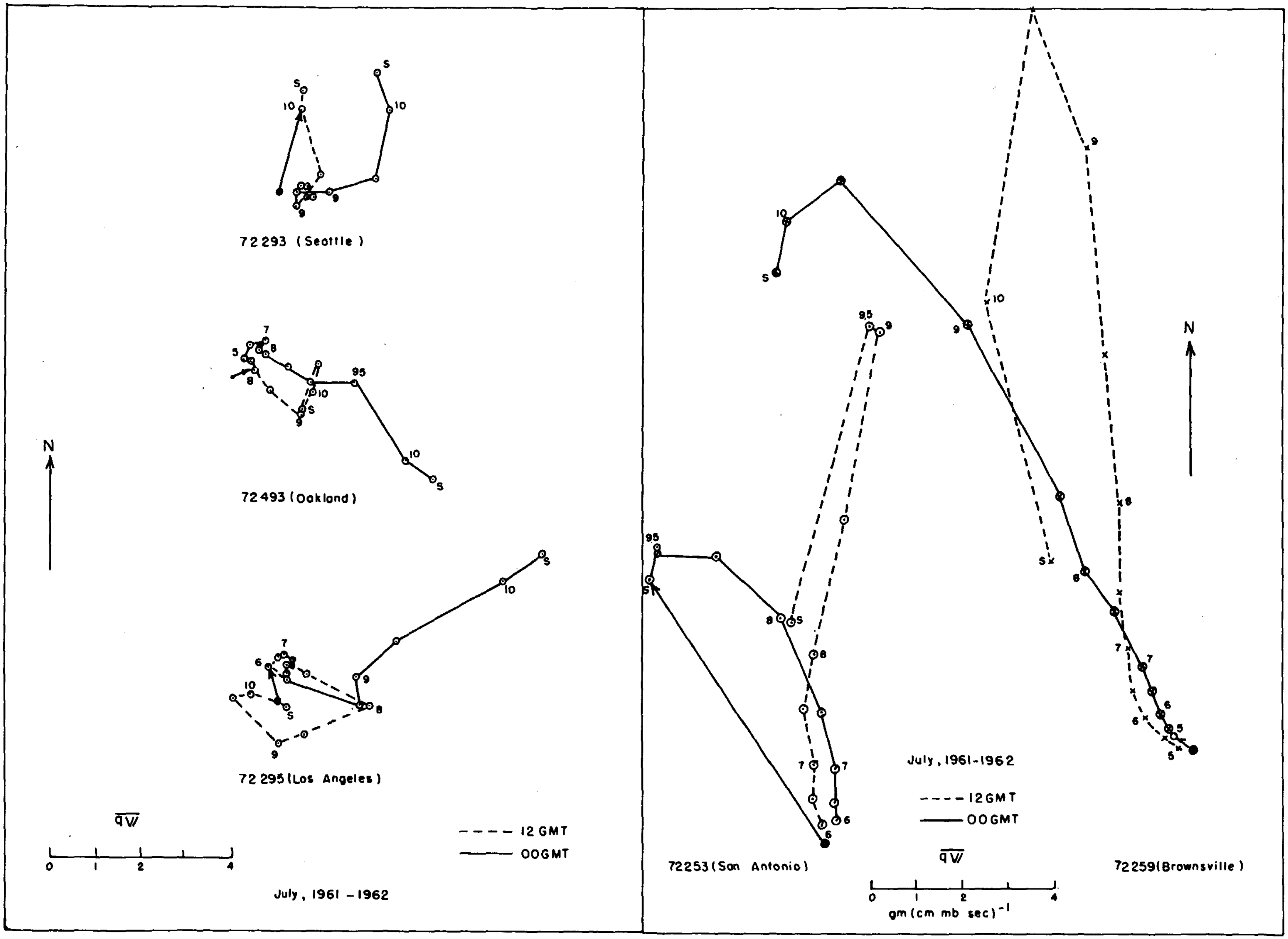

FIGURE 25.—Hodographs: $\overline{q\mathbf{V}}$, for Seattle, Oakland, Los Angeles, San Antonio, and Brownsville, July 1961–62. Origin denoted by solid circle. Pressure given in hundreds of millibars. "S" denotes surface value.

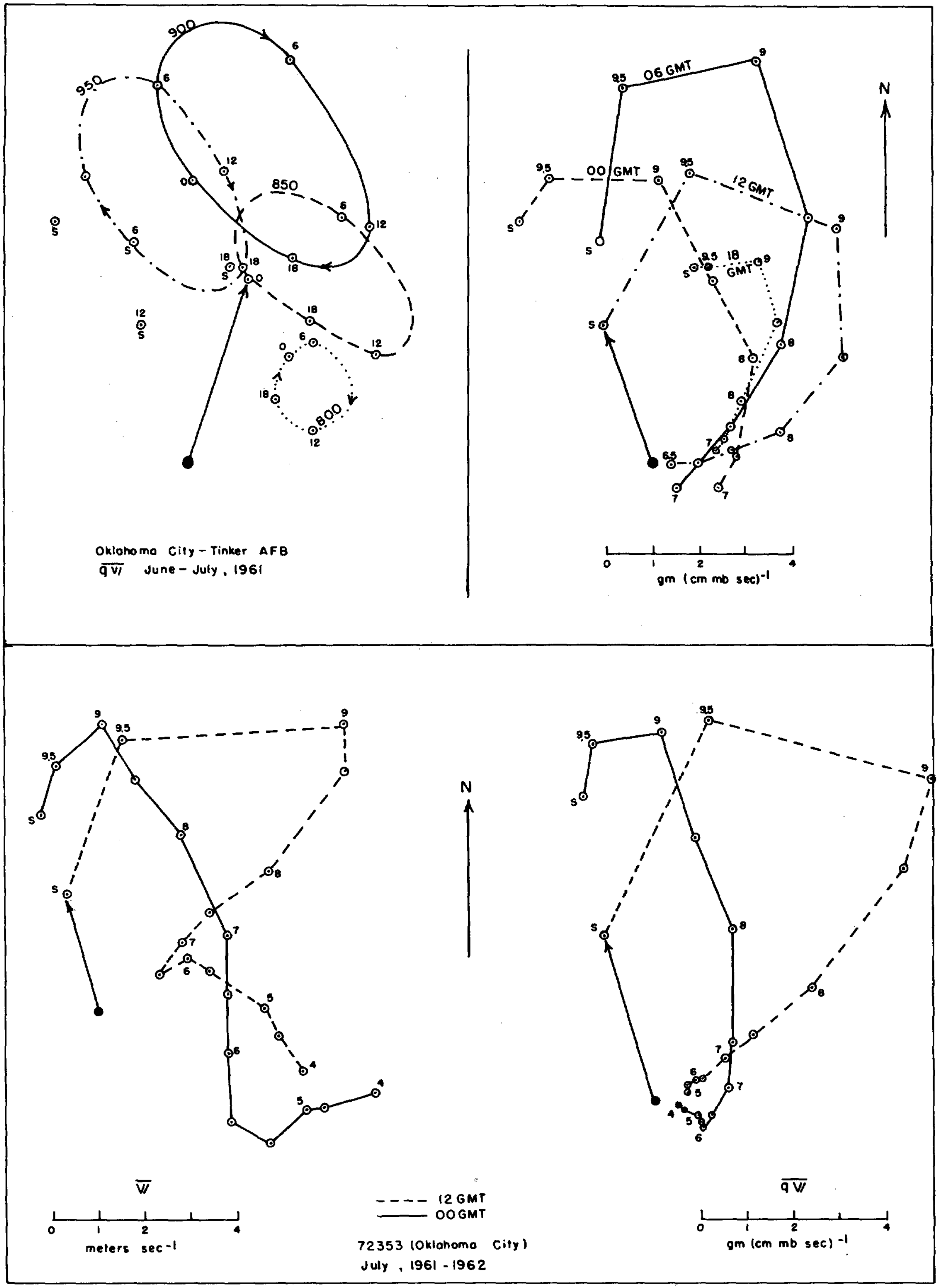

FIGURE 26.—Hodographs: $q\mathbf{V}$ and $\overline{\mathbf{V}}$ for Oklahoma City and Tinker Air Force Base. Upper left: diurnal variations surface–800 mb. GMT observation times noted. Data for June–July 1961 (00 and 12 GMT at Oklahoma City; 06 and 18 GMT at Tinker AFB). Upper right: $\overline{q\mathbf{V}}$, Oklahoma City and Tinker AFB. Lower: $\overline{q\mathbf{V}}$ and $\overline{\mathbf{V}}$, for Oklahoma City, July 1961–62. Origin is denoted by a solid circle. Pressure is given in hundreds of millibars. "S" denotes surface value.

above 650 mb. Changes of this type, characterized by an opposite diurnal turning of the vectors in the lower and middle troposphere, are also typical of region C.

Region C includes eastern Mexico, the western Gulf of Mexico, and most of the United States east of the Continental Divide and south of 42.5° N. Hodographs from that part of the area in which the oscillation is most strongly developed, denoted as sub-area C_1, are illustrated by Merida, figure 24, and the Brownsville and San Antonio hodographs of figure 25. The diurnal changes which are exhibited by these hodographs are quite remarkable, and have two distinct characteristics: (1) a region in the lower troposphere in which $\overline{q\mathbf{V}}$ and $\overline{\mathbf{V}}$ turn anticyclonically between 00 and 12 GMT, surmounted by a region in which the vectors turn cyclonically during the same period; (2) the appearance of a mean low-level jet in the vertical profiles, 50 to 100 mb. above the surface, at 12 GMT. It should be emphasized that the low-level jet of this discussion refers to a maximum in the vertical profiles and not in the horizontal plane. The region of anticyclonic turning does not always extend to the surface. The mean low-level jet appears to be most strongly developed in the region extending from the lower Rio Grande Valley northward through northeastern Texas and Arkansas. The details of the oscillation cannot be determined south of the Rio Grande; however the very large diurnal variations at Merida suggest that this regime extends at least as far south as the Yucatan peninsula.

Observations taken four times daily by the Oklahoma City (00–12 GMT)–Tinker Air Force Base (06–18 GMT) combination allow one to obtain a somewhat better picture of the behavior of the oscillation in that particular area. These stations are only a few miles apart and at practically the same elevation (surface pressure approximately 970 mb.). Data were available from both stations for June and July 1961, and hodographs for this period, for the four observation times, are shown in figure 26. Also sketched are the oscillations at the 950, 850, and 800-mb. levels. No reasonable curve could be sketched from the surface observations, possibly because of local differences between the two stations. Analysis of several additional winter months indicated the presence, in addition to the diurnal oscillations, of an unexplained systematic difference between the mean monthly winds at the two stations, which in turn masks the weaker oscillations above 800 mb.

The characteristic features of region C_1 hodographs are found over the remaining portions of region C, although the boundary between the cyclonic and anticyclonic changes is not always as clear cut as in C_1, and the low-level jet is not so well developed.

Region D includes those stations which exhibit a mixture of the characteristics of regions A and C. A mean 12 GMT low-level jet is found at the northerly stations, but unlike in region C, this development is accompanied by a cyclonic turning of the flux vector. The southerly stations exhibit the increased 12 GMT southerly flow typical of region A, but the hodographs are quite dissimilar in other respects.

Region E includes the area west of the Continental Divide, exclusive of the Pacific coast. The hodographs are strongly influenced by local conditions, which make it difficult to isolate the significant large-scale features.

Stations on the Pacific Coast (region F) exhibit a great deal of diurnal variability in the lower levels, since the 00 GMT observation coincides closely with the time of maximum sea breeze development. The strong sea breeze regimes of San Francisco Bay and the Los Angeles Basin show up strongly on the Los Angeles and Oakland hodographs (fig. 25).

Over Canada and the northern United States, even in July, the amplitude of the oscillations is quite small. Thus, it is probably necessary to analyze a longer period of data before drawing firm conclusions concerning this area.

Some idea of the broadscale characteristics of the well organized diurnal circulation system over the Central American Sea and the area east of the Rockies and south of 42° N. can be obtained from figures 27 and 28. Figure 27 shows the mean low-level departure vector field during July. Where the mean surface pressure is greater than 950 mb., the vector is derived from an average of the 900- and 950-mb. winds; otherwise the average of the winds at the first two standard 50-mb. levels above the surface is used. Figure 28 shows the mean mid-tropospheric departure vector field derived from an average of the winds at 500 and 550 mb. The heavy solid line on each chart indicates the position of a prominent low-level mean monthly streamline around the subtropical High, obtained by averaging the 00 and 12 GMT observations. These maps have counterparts in figures 6 and 7 of Hering and Borden [12], which are based on July 1958 data from only the United States. Where comparisons can be made, the departure vectors are usually in excellent agreement.

The characteristic features of the hodographs of regions A through D can now be summarized in terms of a large-scale diurnal circulation system. Comparison of figures 27 and 31 shows the veering of the low-level wind between 00 and 12 GMT in region C to be the manifestation of an oscillation that occurs in the regions bordering the western extension of the subtropical High. If one directs his attention to that portion of the low-level streamline extending from the Yucatan peninsula to the Atlantic Coast, it is seen that the relationship of the low-level departure vectors to the streamline is such as to give relative inflow to the region of high pressure at 12 GMT. On the other hand, a similar comparison for the mid-troposphere (fig. 28) shows the departure vectors crossing the mean streamline in the opposite direction; consequently the departure vectors in the low- and mid-troposphere are sharply out of phase. Careful examination of these departure fields strongly suggests relative low-tropospheric convergence and mid-

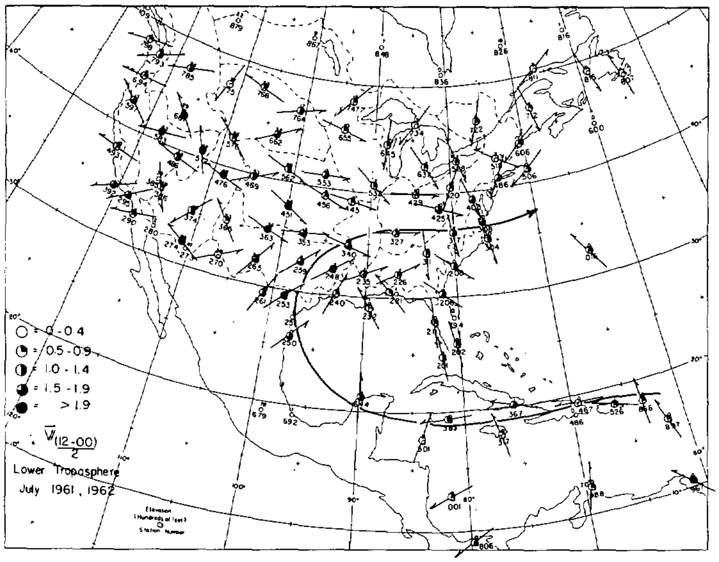

FIGURE 27.—Difference, (12–00 GMT)/2, of the average of the wind at the first two standard levels (50-mb. intervals) above the ground, July 1961–62. Units: m. sec.$^{-1}$

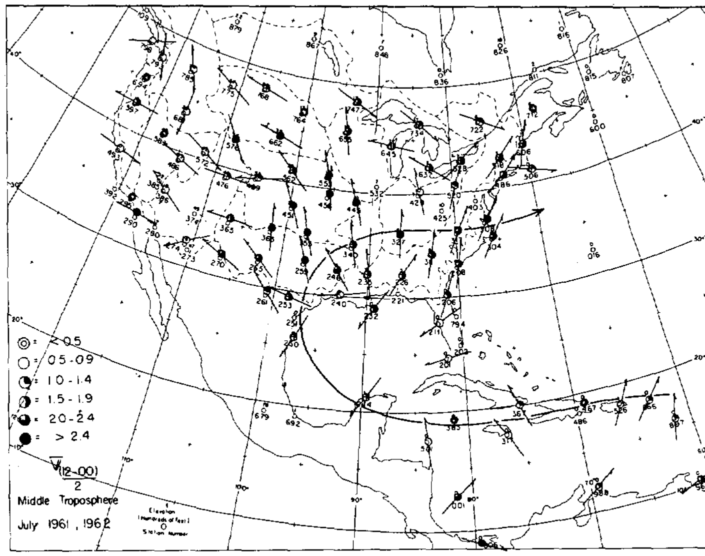

FIGURE 28.—Difference, (12–00 GMT)/2, of the average of the wind at 500 and 550 mb., July 1961–62. Units: m. sec.$^{-1}$

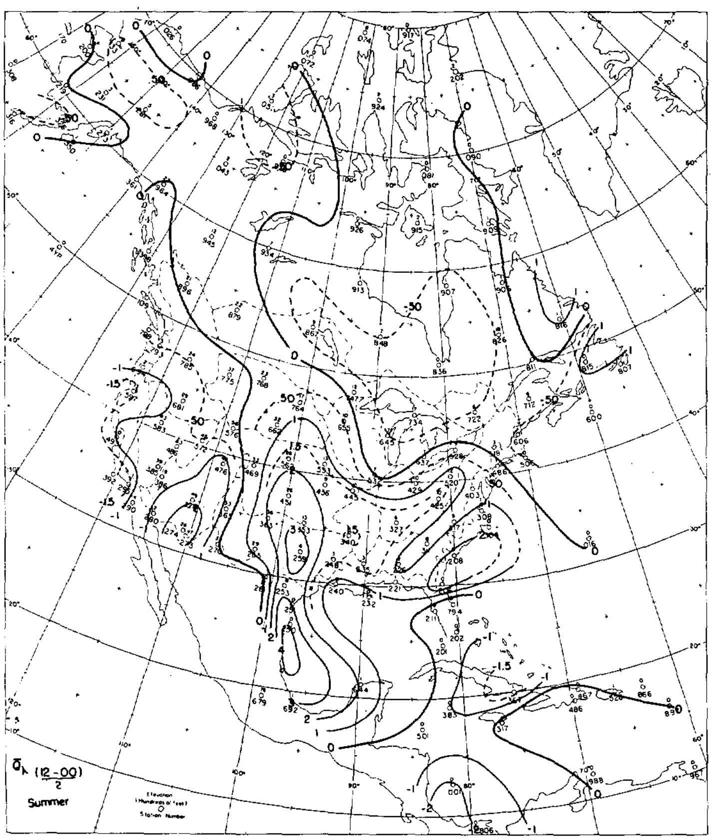

FIGURE 29.—Difference, (12–00 GMT)/2, of the vertically integrated mean total zonal water vapor flux, June–August, 1961–62. Units: 10^2 gm. (cm. sec.)$^{-1}$.

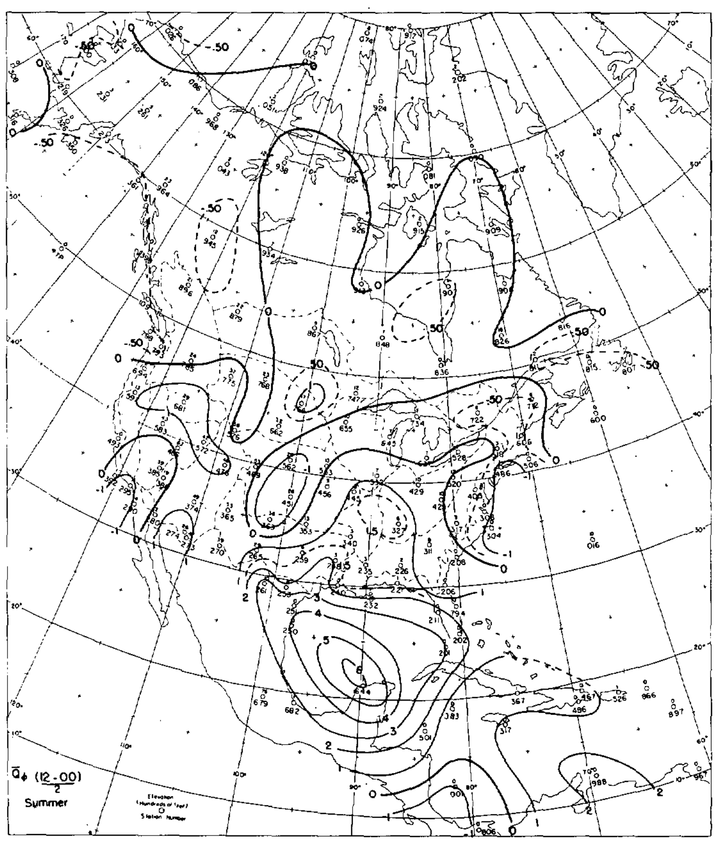

FIGURE 30.—Same as figure 29, but for the vertically integrated mean total meridional water vapor flux.

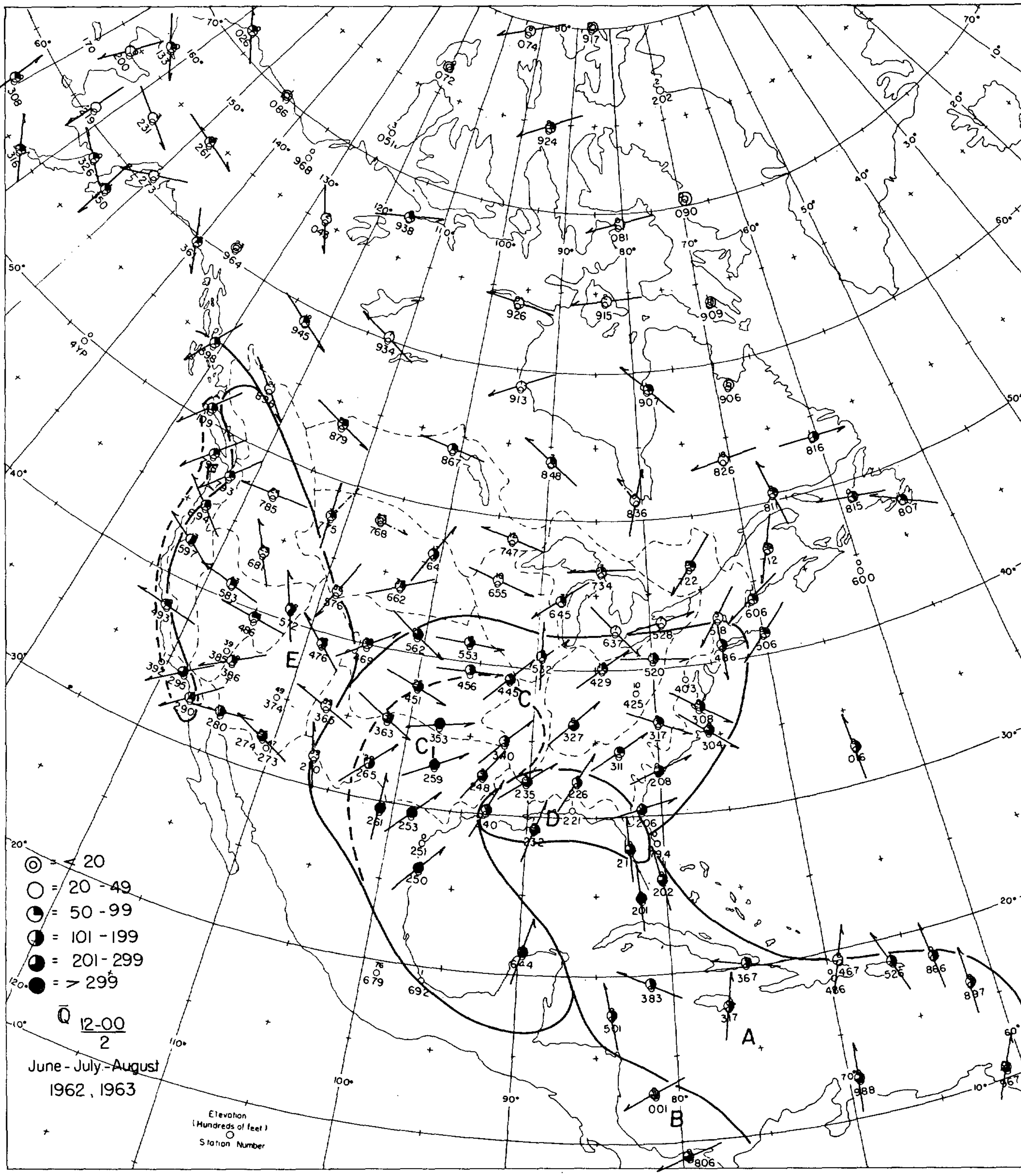

FIGURE 31.—Difference, (12–00 GMT)/2, of the vertically integrated mean total water vapor flux vector, June–August, 1961–62. Units: gm. (cm. sec.)$^{-1}$. Designated regions are those in which flux variations exhibit similar characteristics.

tropospheric divergence at 12 GMT (with the reverse pattern at 00 GMT) within the region enclosed by the mean streamline and west of approximately 82° W. The "Hering-Borden" oscillation of the mid-troposphere and the low-level oscillation thus appear to be highly divergent compensating departures from the mean flow. Discussion of the diurnal variations in the divergence field of $\overline{\mathbf{V}}$ and $\overline{q\mathbf{V}}$ will be deferred to Part II of this summary; however it can be stated that limited analysis of the $\overline{\mathbf{V}}$ fields, and implications from extensive analyses of $\nabla\cdot\overline{\mathbf{Q}}$ (see Rasmusson [24]) support the above speculations.

The complications which these diurnal variations introduce into any study of the atmospheric vapor flux, or, for that matter, in many other types of observational studies, is quite apparent.

DIURNAL CHANGES IN THE VERTICALLY INTEGRATED VAPOR FLUX

Some idea of the extent and magnitude of the summertime oscillations in the mean total vertically integrated vapor flux can be obtained from figures 29 and 30, which show the difference between the 12 GMT and 00 GMT values of $\overline{Q}_\phi$ and $\overline{Q}_\lambda$ for the period June-August, 1961 and 1962. The details of the oscillation cannot, of course, be determined from twice daily observations. However, the data from Fort Worth and Oklahoma City, and the results of Hering and Borden [12], indicate that the oscillations are roughly elliptic, with axes of the same order of magnitude. Thus the vector defined by the component maps can be used as a rough estimate of the amplitude of the oscillation. These vectors are shown in figure 31. The magnitude of the flux variations may be compared with the 00 GMT July flux shown in figures 5 and 6.

The pattern obtained from the data is quite coherent, even over those areas where values are small. Only station 72836 (Moosinee) was ignored in the analysis; this because of apparently unrepresentative data for 00 GMT, August 1961. In addition, data from three other stations were smoothed on one or more individual monthly analyses. The (12−00)/2 difference vector computed from the smoothed analysis is also shown at the appropriate stations on figure 31. These adjustments produce changes in detail only.

Analyses of individual monthly maps (not shown here) indicate the same general pattern each month south of 45° N., but farther north where the magnitude of the oscillations is small, the pattern is more variable from month to month, particularly in the meridional component. As would be expected from the previous discussion, the diurnal change is particularly pronounced around the western Gulf of Mexico, where Merida, on the Yucatan peninsula, consistently shows the greatest changes on the map. This results in a substantial increase between 00 and 12 GMT in the northward flux from the Gulf of Mexico (see figs. 32, and 22, lower left).

The summertime diurnal variations of the zonal flux form an interesting pattern over the United States and

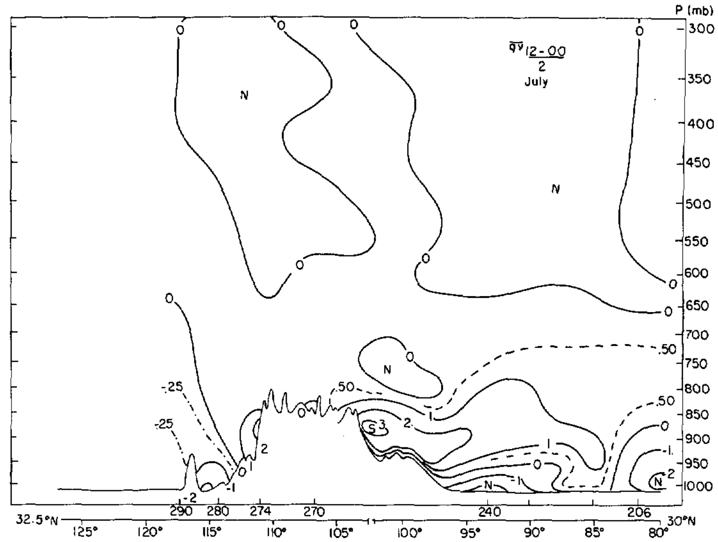

FIGURE 32.—Difference, (12–00 GMT)/2, of the mean total meridional water vapor flux, July 1961–62. 30° N.; 80° W.–105° W. and 32.5° N.; 105° W.–117.5° W. Units: gm. (cm. mb. sec.)$^{-1}$.

southern Canada. Over extreme western Canada and the western United States, the eastward component decreases between 00 and 12 GMT, thus giving a relative offshore flow along the west coast at 12 GMT. The eastern boundary of this regime coincides roughly with the Continental Divide. The 12 GMT transport is relatively eastward between the Rocky Mountains and the east coast south of 42.5° N., and over a rather narrow region extending northwestward just to the east of the Canadian Rockies. The oscillations over this region are most pronounced between the Rocky Mountains and Appalachians, and along the southeastern coast. The third major region is one of increased westward flow at 12 GMT, and extends westward from Newfoundland through the Great Lakes, Hudson Bay, and northwestward to the vicinity of the Great Slave Lake.

The difference between the 12 GMT and 00 GMT mean flux for the three winter months (December, January, February) is shown in figures 33 and 34. The patterns are much weaker than those found during summer. The main features of the summer zonal oscillations are still identifiable, but the meridional component is similar only south of 30° N.

In summary, the observed diurnal oscillations of the wind, and, as a consequence, the mean monthly diurnal oscillations of the water vapor transport over North America and the Central American Sea, appear to be produced by a combination of local and large-scale effects. At stations in the western United States, the diurnal changes are mostly local in nature, although there is some indication of a weak large-scale circulation (relatively westward at 12 GMT). East of the Continental Divide, and south of 42° N., the local oscillations fit into a beautifully organized large-scale diurnal circulation pattern. It will be shown in

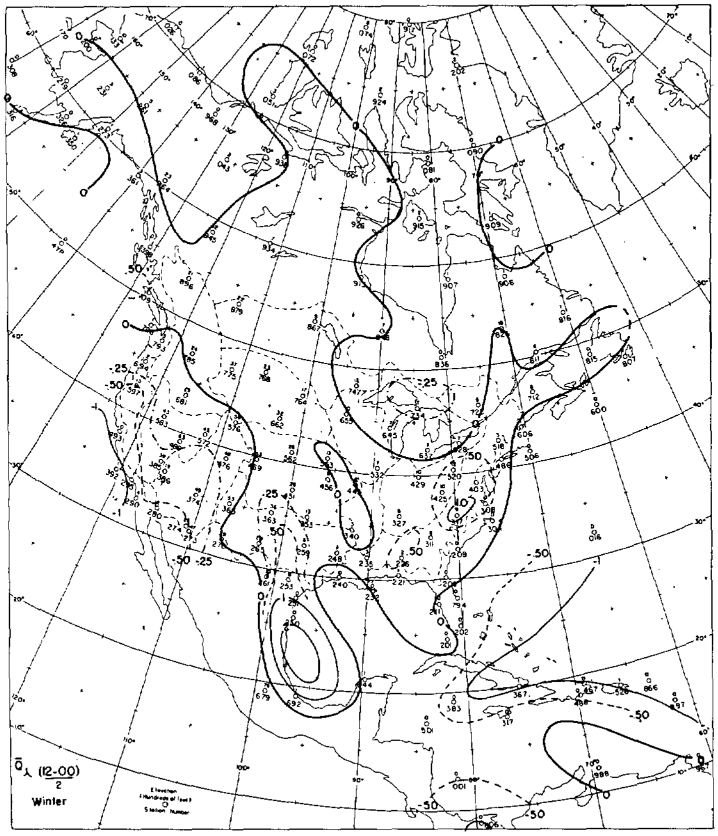

FIGURE 33.—Difference, (12–00 GMT)/2, of the vertically integrated mean total zonal water vapor flux, December–February, 1961–62 and 1962–63. Units: 10^2 gm. (cm. sec.)$^{-1}$.

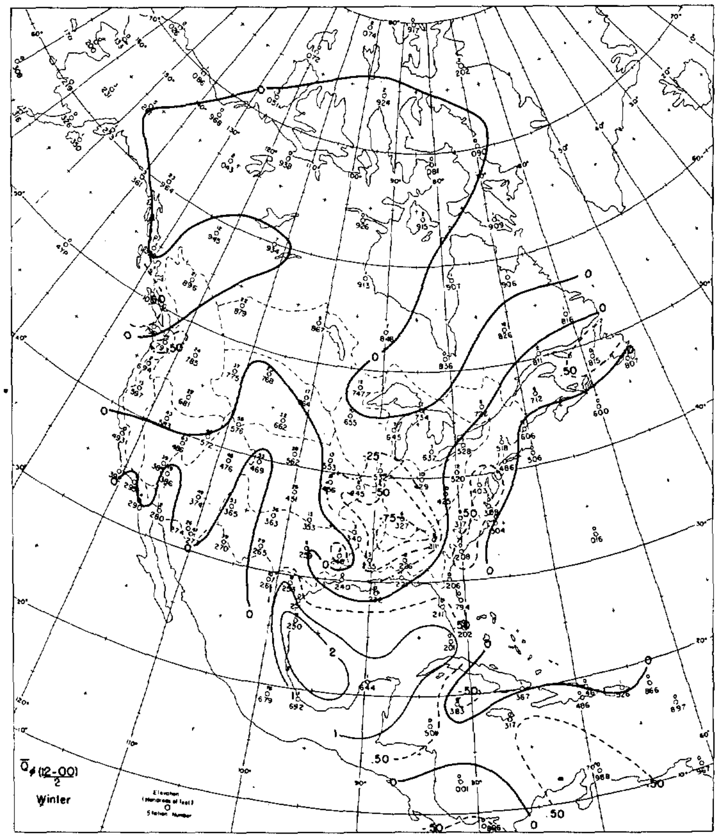

FIGURE 34.—Same as figure 33, but for the vertically integrated mean total meridional water vapor flux.

Part II that these variations in the flux field produce significant diurnal variations in the flux divergence as well.

Because of the apparent relationship of these oscillations to the large-scale flow pattern over eastern North America, one would expect changes in detail from year to year. Preliminary analysis of additional data from Fort Worth, the findings of Hering and Borden [12], and results of flux divergence computations over eastern North America (to be discussed in Part II) indicate this to be true.

5. SUMMARY

The fields of mean total water vapor flux over North America and the Central American Sea during the period May 1, 1960–April 30, 1963, have been studied both in terms of mean annual characteristics and seasonal variations. Important aspects of the regional climatology of the vapor flux are illustrated by maps and cross sections and through computations, on a mean monthly basis, of the total vapor flux across selected boundaries.

This paper is to a large extent a revision and extension of a portion of the earlier work of Benton and Estoque [2]. Specifically, (1) the region has been enlarged to include the Central American Sea; (2) the resolution has been greatly increased through the use of data at 50-mb. intervals (as opposed to data from only mandatory levels) from a much improved network of stations; (3) actual winds, rather than geostrophic, are used; (4) the period of investigation covers two years. Using these data, one can determine more accurately, and in somewhat more detail, the important features of the flux field. It is primarily in such details as, for instance, the slopes of the various flux maxima with height, their intensities, and the vertical distribution of the flux, particularly across 30° N., that the results of this study differ from those of Benton and Estoque. The major features of the North American flux field which they described are essentially confirmed. One of the more significant differences is found along the southwestern border of the United States, where their data apparently were not sufficient to define the weak maximum of summertime northward flux into the Colorado Basin.

Of considerable significance to vapor flux studies in particular, and perhaps to observational studies in general, is the finding that diurnal variations in the mean monthly wind field produce significant diurnal variations in the transport of water vapor, particularly during summer south of 50° N. The existence of significant variations in the mean monthly wind field over the central United States has previously been noted by Hering and Borden [12]. The results of this investigation indicate that the variations over the central United States constitute only a part of a much larger diurnal wind system which extends over portions of Mexico and the Central American Sea, as well as over most of the eastern United States.

Finally, the irregular variation of the total mean monthly flux through several of the boundaries calls for the analysis of a longer period of record in order to firmly establish the important features of the seasonal pattern, and to obtain an estimate of the variability of this pattern. Along the same line, significant differences were observed in certain details of the mean annual flux fields between the first and second year, particularly over eastern North America and the Central American Sea. These will be discussed in Part II, but it should be noted that such interannual changes also point up the desirability of analyzing a longer period of record.

ACKNOWLEDGMENTS

The author is deeply indebted to Professor Victor P. Starr for his constant interest, guidance, and encouragement during the course of the investigation. The helpful suggestions of Dr. José Peixoto and Dr. Paul Bock during the initial stages of the investigation were very much appreciated. The author would also like to thank Dr. E. Kung for reviewing the original manuscript.

The massive amount of data processing required for this investigation was accomplished through the efforts of a number of people: Mr. Howard Frazier and Mr. Raymond Ellis of Travelers Research Center, Mr. Salmon P. Seroussi of Mitre Corporation, and Mrs. Judy Copeland and Miss Judy Roxborough of M.I.T. Calculations were performed at the Geophysical Fluid Dynamics Laboratory, Mitre Corporation, and the M.I.T. Computation Center.

Mr. William Schallert of the Environmental Data Service, ESSA, is to be thanked for providing a certain amount of additional flux data.

Credit for construction of the cross sections goes to Maj. Merwin Richards, Capt. David Feruzza, and Mr. Troop Berg, and the author is grateful for their use.

The help of Miss Isabelle Kole in drafting the figures, and Mrs. C. Bunce in typing the manuscript is appreciated.

The author wishes to express his appreciation to ESSA, and particularly to Dr. Joseph Smagorinsky, for the opportunity to perform this investigation.

The research was made possible through the support of the National Science Foundation under grant numbers GP-820 and GP-3657. Additional support was received from the U.S. Air Force 433-L Program and Mitre Corporation.

REFERENCES

1. G. S. Benton, R. T. Blackburn, and V. O. Snead, "The Role of the Atmosphere in the Hydrologic Cycle," *Transactions of the American Geophysical Union*, vol. 31, No. 1, Feb. 1950, pp. 61-73.
2. G. S. Benton and M. A. Estoque, "Water Vapor Transfer over the North American Continent," *Journal of Meteorology*, vol. 11, No. 6, Dec. 1954, pp. 462-477.
3. G. S. Benton, M. A. Estoque, and J. Dominitz, "An Evaluation of the Water Vapor Balance of the North American Continent," *Scientific Report No. 1*, Contract No. AF19-122-365, Johns Hopkins University, July 1953, 101 pp.
4. A. K. Blackadar, "Boundary Layer Wind Maxima and Their Significance for the Growth of Nocturnal Inversions," *Bulletin of the American Meteorological Society*, vol. 38, No. 5, May 1957, pp. 283-290.
5. W. Bleeker and M. J. Andre, "On the Diurnal Variation of Precipitation, Particularly over the Central U.S.A.," *Quarterly Journal of the Royal Meteorological Society*, vol. 77, No. 332, Apr. 1951, pp. 260-271.
6. M. I. Budyko, *Atlas Teplovogo Balansa Zemnogo Shara*, Glavnaíâ Geofizicheskaíâ Observatoriíâ, USSR, 1963, 69 pp. (Text translated by I. A. Donehoo as "Guide to the Atlas of the Heat Balance of the Earth"; U.S. Weather Bureau, Washington, D.C.).
7. R. C. Curtis and H. A. Panofsky, "The Relation Between Large Scale Vertical Motion and Weather in Summer," *Bulletin of the American Meteorological Society*, vol. 39, No. 10, Oct 1958, pp. 521-531.
8. F. Defant, "Local Winds," *Compendium of Meteorology*, American Meteorological Society, Boston, 1951, pp. 655-672.
9. J. R. Gerhardt, "An Example of a Nocturnal Low-Level Jet," *Journal of the Atmospheric Sciences*, vol. 19, No. 1, Jan. 1962, pp. 116-118.
10. M. F. Harris, "Diurnal and Semi-Diurnal Variations of Wind, Pressure, and Temperature in the Troposphere over Washington, D.C.," *Journal of Geophysical Research*, vol. 64, No. 8, Aug. 1959, pp. 983-995.
11. S. L. Hastenrath, "The Flux of Atmospheric Water Vapor over the Caribbean Sea and the Gulf of Mexico," *Journal of Applied Meteorology*, vol. 5, No. 6, Dec. 1966, pp. 778-788.
12. W. S. Hering and T. R. Borden, Jr., "Diurnal Variations in the Summer Wind Field over the Central U.S.," *Journal of the Atmospheric Sciences*, vol. 19, No. 1, Jan. 1962, pp. 81-86.
13. W. H. Hoecker, Jr., "Three Southerly Low-Level Jet Systems Delineated by the Weather Bureau Special Pibal Network of 1961," *Monthly Weather Review*, vol. 91, No. 10-12, Oct.-Dec. 1963, pp. 573-582.
14. W. H. Hoecker, Jr., "Comparative Physical Behavior of Southerly Boundary-Layer Wind Jets," *Monthly Weather Review*, vol. 93, No. 3, Mar. 1965, pp. 133-144.
15. B. Holzman, "Sources for Moisture for Precipitation in the United States," *Technical Bulletin No. 589*, Dept. of Agriculture, Washington, D.C., 1937.
16. J. W. Hutchings, "Water Vapor Flux and Flux Divergence over Southern England: Summer 1954," *Quarterly Journal of the Royal Meteorological Society*, vol. 83, No. 1, Jan. 1957, pp. 30-48.
17. J. W. Hutchings, "Water-Vapor Transfer over the Australian Continent," *Journal of Meteorology*, vol. 18, No. 5, Oct. 1961, pp. 615-634.
18. Y. Izumi, "The Evolution of Temperature and Velocity Profiles during the Breakdown of a Nocturnal Inversion and a Low-Level Jet," *Journal of Applied Meteorology*, vol. 3, No. 1, Feb. 1964, pp. 70-82.
19. Y. Izumi and M. Barad, "Wind and Temperature Variations during Development of a Low-Level Jet," *Journal of Applied Meteorology*, vol. 2, No. 5, Oct. 1963, pp. 668-673.
20. J. D. Kiamal and Y. Izumi, "Vertical Velocity Fluctuations in a Nocturnal Low-Level Jet," *Journal of Applied Meteorology*, vol. 4, No. 5, Oct. 1965, pp. 576-584.
21. E. Palmén, "Computation of the Evaporation over the Baltic Sea from the Flux of Water Vapor in the Atmosphere," *International Association of Scientific Hydrology, Publication No. 62*, 1963, pp. 244-252.

22. J. P. Peixoto and A. R. Crisi, "Hemispheric Humidity Conditions During the IGY," *Scientific Report No. 6*, Planetary Circulations Project, Massachusetts Institute of Technology, Nov. 1965, 166 pp.
23. E. M. Rasmusson, "Diurnal Variations in the Summer Water Vapor Transport over North America," *Water Resources Research*, vol. 2, 3d Quarter 1966, pp. 469–477.
24. E. M. Rasmusson, "Atmospheric Water Vapor Transport and the Hydrology of North America," *Report No. A-1*, Planetary Circulations Project, Massachusetts Institute of Technology, May 1966, 170 pp.
25. V. P. Starr and R. M. White, "Direct Measurement of the Hemispheric Poleward Flux of Water Vapor," *Journal of Marine Research*, vol. 14, No. 2, 1955, pp. 217–225.
26. V. P. Starr and J. P. Peixoto, "On the Global Balance of Water Vapor and the Hydrology of Deserts," *Tellus*, vol. 10, No. 2, May 1958, pp. 189–194.
27. V. P. Starr, J. P. Peixoto, and A. R. Crisi, "Hemisphere Water Balance for the IGY," *Tellus*, vol. 17, No. 4, Nov. 1965, pp. 463–472.
28. H. Wexler, "A Boundary Layer Interpretation of the Low-Level Jet," *Tellus*, vol. 13, No. 3, Aug. 1961, pp. 368–378.
29. R. M. White, "The Meridional Eddy Flux of Energy," *Quarterly Journal of the Royal Meteorological Society*, vol. 77, No. 332, Apr. 1951, pp. 188–199.
30. G. Wüst, *Stratification and Circulation in the Antillean-Caribbean Basins*, Columbia University Press, New York, 1964, 201 pp.

[*Received March 30, 1967; revised May 4, 1967*]